



Cite this: *Lab Chip*, 2015, 15, 3439

The Poisson distribution and beyond: methods for microfluidic droplet production and single cell encapsulation

David J. Collins,^{*a} Adrian Neild,^b Andrew deMello,^c Ai-Qun Liu^d and Ye Ai^{*a}

There is a recognized and growing need for rapid and efficient cell assays, where the size of microfluidic devices lend themselves to the manipulation of cellular populations down to the single cell level. An exceptional way to analyze cells independently is to encapsulate them within aqueous droplets surrounded by an immiscible fluid, so that reagents and reaction products are contained within a controlled microenvironment. Most cell encapsulation work has focused on the development and use of passive methods, where droplets are produced continuously at high rates by pumping fluids from external pressure-driven reservoirs through defined microfluidic geometries. With limited exceptions, the number of cells encapsulated per droplet in these systems is dictated by Poisson statistics, reducing the proportion of droplets that contain the desired number of cells and thus the effective rate at which single cells can be encapsulated. Nevertheless, a number of recently developed actively-controlled droplet production methods present an alternative route to the production of droplets at similar rates and with the potential to improve the efficiency of single-cell encapsulation. In this critical review, we examine both passive and active methods for droplet production and explore how these can be used to deterministically and non-deterministically encapsulate cells.

Received 3rd June 2015,
Accepted 21st July 2015

DOI: 10.1039/c5lc00614g

www.rsc.org/loc

^a *Engineering Product Design pillar, Singapore University of Technology and Design, Singapore. E-mail: david_collins@sutd.edu.sg, aiye@sutd.edu.sg*

^b *Department of Mechanical and Aerospace Engineering, Monash University, Clayton, VIC 3800, Australia*

^c *Department of Chemistry and Applied Biosciences, Institute of Chemical and Bioengineering, ETH Zürich, Vladimir Prelog Weg 1, 8093 Zürich, Switzerland*

^d *School of Electrical & Electronic Engineering, Nanyang Technological University, 50 Nanyang Avenue, 639798, Singapore*

1 Introduction

Cellular analysis is a major application of microfluidic systems, whose dimensions permit the on-chip culturing and manipulation of cells using geometries and externally applied force fields with length scales comparable to the cells themselves.^{1,2} To support the controlled manipulation of cells in a



David J. Collins

manipulation, especially using high-frequency acoustic fields.

David Collins is a Postdoctoral Researcher at the Singapore University of Technology and Design since 2015. He received his PhD in acoustic microfluidics from Monash University in 2015, including the Bill Melbourne award for best thesis, and his bachelor degree in Biomedical Engineering from the University of Melbourne in 2010. David's current research is on the development of high-speed microfluidic actuation systems for cell



Adrian Neild

microsystems, including microsensors and microfluidics. Recently, he has been working on applying acoustic forcing mechanisms in two phase microfluidic systems.

Adrian Neild is an Australian Research Fellow and Associate Professor at Monash University. He received a Ph.D. in Engineering from the University of Warwick in 2003. Subsequently, he worked as a postdoctoral researcher at the Institute for Mechanical Systems at the Swiss Federal Institute of Technology, Zurich (ETH Zurich). He has been a faculty member at Monash University since 2006; his research interests are in

high-throughput manner, a wide suite of methods have been developed to localize, lyse, electroporate, fuse, sort, concentrate, and mix cells with reagents. From a research standpoint, the predominant paradigm in which cells are suspended within a single flowing aqueous phase in a system of microchannels, has been a highly successful one, with thousands of researchers continuing to be actively engaged in this field,³ producing useable devices for applications including HIV detection,⁴ cancer screening⁵ and the organ-on-a-chip.^{6,7} However, despite the advantages conferred by operating at the microscale, many of these systems suffer from the same issues as those at larger length scales, though the physical process may differ; *e.g.* undesired mixing and concentration gradients can result from diffusion instead of advective transport. Furthermore, as the dimensions of a microchannel approaches that of a cell, stiction and cell adhesion to channel walls severely limits the reusability of

such devices or restricts the types of on-chip cell culturing that can be performed.

Such restrictions, especially the inability to reliably inhibit diffusive mixing over long time scales, prevent the use of single-phase systems for many applications in the growing field of single-cell analysis. Here, single cells are assayed on an individual, rather than the population basis. This is critically important as the phenotypic expression of cells can vary substantially in a cell population with identical genotypes; a good example being the somatic cell population that makes up a variety of human body tissues. Even within the same tissue cells exhibit a range of epigenetic factors, as each experiences a unique microenvironment that influences their development and function.⁸ By inspecting the relevant parameters of each cell individually, whether that be *via* a fluorescent reporter, inferred physical dimension or electrical/mechanical property, the degree of heterogeneity in a cell population can be determined.^{9–14} Heterogeneity is known to play a key role in the development of some tumors¹⁵ in addition to applications such as the discovery of rare cells¹⁶ and high-throughput screening,¹⁷ where the influence of the local microenvironment can also be assessed by altering its constituent concentrations.¹⁸

Traditionally, the study of individual cells utilizes some combination of flow cytometry and downstream processing, often *via* fluorescence activated cell sorting (FACS).^{19,20} In flow cytometry a sample stream containing cells is hydrodynamically focused into a line of single cells, which can then be independently inspected *via* optical or impedance measurement.^{21,22} While flow cytometry is successful as a single-cell measurement system, where individual cells can be screened at high-throughput, as traditionally performed (in a single fluid phase) it is limited to applications where inter-cellular interaction is tolerable and poor control of the local environment is an acceptable constraint. In a single-fluid phase, the environment is controlled at a global level but



Andrew deMello

Andrew deMello is Professor of Biochemical Engineering in the Department of Chemistry and Applied Biosciences at ETH Zürich. Between 1997 and 2011 Andrew was Professor of Chemical Nanosciences in the Chemistry Department at Imperial College London. He has given over 250 invited lectures worldwide, published over 230 papers in the areas of microfluidics and nano-scale science, and co-authored two books.



Ai-Qun Liu

Dr Ai-Qun Liu (A. Q. Liu) is currently Professor at the School of Electrical & Electronic Engineering, Nanyang Technological University, Singapore. He serves as editor and editorial board member of more than 10 scientific journals. He is the author or co-author of over 200 publications and peer-reviewed journal papers and author of two books. He won the Institute of Engineering Singapore (IES) Award in 2006 and the University Scholar

award in 2007. He specializes in the research fields of MEMS and optofluidics.



Ye Ai

Ye Ai is an Assistant Professor at Singapore University of Technology and Design (SUTD) since 2013. He received his B.S. in Mechanical Engineering from Huazhong University of Science and Technology in 2005, and his Ph.D. in Mechanical and Aerospace Engineering from Old Dominion University in 2011. Prior to joining SUTD, he worked as a postdoctoral researcher at the Bioscience Division of Los Alamos National

Laboratory. He was a visiting professor at Massachusetts Institute of Technology from August 2014 to July 2015. His research interest focuses on developing novel microfluidic technologies for particle/cell manipulation and single cell analysis.

uncontrolled in the immediate locality of an individual cell, meaning that any measurement of the extracellular environment is on a population rather than a single-cell basis. In a single phase system, the isolation of a cell's microenvironment can be accomplished through the use of pneumatically actuated chambers,^{23,24} although it is difficult to integrate more than a few such (independently controlled) reaction chambers on a single device.

There are a number of applications where a cell must be locally contained to control intercellular interactions and cell signalling. 3D tissue printing requires meticulous control of the cell environment in order to direct cell growth and cell fate, often through the use of hydrogel capsules and changes in the mechanical or chemical properties of the extra-cellular matrix,^{25–27} though two-phase bioprinting presents another route to preventing cell–cell interaction.^{28,29} The artificial pancreas, for example, makes use of encapsulated islet cells to limit immune system response post-implantation.^{30–32} Conversely, it can be desirable to interact specific cells, such as in cell fusion for hybridoma formation, cell reprogramming, and antibiotic drug discovery, activities that require fine-grained control of a cell's position and environment,^{33–35} abilities also required in studies on protein expression and antibody production.^{36,37}

An evolving methodology to control the cellular environment makes use of the principles of droplet-based microfluidics, where an aqueous flow is segmented into individual droplets within an immiscible carrier fluid (often a mineral

or fluorinated oil) to encapsulate cells, organic molecules and reagents.^{37–43} This concept for single-cell analysis is explored in Fig. 1. Here, some of the numerous advantages associated with the encapsulation of cells within droplets are evident. First, as the oil–water interface provides a natural barrier to diffusion, cellular products remain contained in its immediate vicinity, so that even significant concentration gradients between droplets can be maintained and dilution minimized.⁴⁴ Second, the reaction volume is significantly reduced when compared to single-phase microfluidic systems, a significant factor when using high-value reagents such as enzymes or DNA. Third, the ability to control the location and duration of discrete fluid volumes is enhanced^{45,46} and long term cell culture is simplified by preventing adhesion between encapsulated cells or to device features.⁴⁷

Two-phase systems can also be utilized with the same versatility as single-phase ones. For example, reagents and other cells can be added using a number of different micro-injection and droplet coalescence techniques.^{45,48–50} Analyte diffusion across the oil–water interface can also be controlled through interface modification to selectively control diffusion between the droplet and its environment^{51–53} or between individual droplets.^{54–57} Moreover, the ability to selectively control diffusion, and merge droplets permits long-term cell viability assessment, as noted in a range of prior studies.^{58–62} Leveraging these advantages has enabled the application of droplet-based encapsulation methods in high throughput drug screening,¹⁷ rare cell detection,⁶³ single-cell DNA amplification,⁶⁴ and directed evolution,^{65–68} in addition to non cell-based applications including the study of crystal growth,^{69,70} single-molecule detection,⁷¹ protein–protein interaction,⁷² nanomaterial synthesis⁷³ and drug delivery.⁷⁴ For a thorough discussion of the advantages that encapsulation confers for single cell analysis, the reader is directed to a number of excellent reviews published elsewhere.^{9,37,75,76}

Cell encapsulation offers substantial benefits for microenvironmental control and sample handling, however significant questions remain regarding the optimal method(s) for encapsulation. That said, systems incorporating microfluidic methods are the most promising, where cell encapsulation is performed reliably through the use of features or force gradients on the scale of the cells themselves. By far, the most common method of encapsulating cells makes use of microfluidic channel geometries that mix co-flowing water and oil phases, where (in most cases) the water phase self-separates into discrete water droplets. Using T-junctions, flow-focusing or co-flowing intersections, droplet formation can be accurately controlled through variation of differential volumetric flow rates of the immiscible fluid phases. However, it is not straightforward to control the number of cells encapsulated on a droplet-by-droplet basis, especially important as one cell per droplet is highly desired for single-cell analysis. If the encapsulation of dispersed cells into droplets occurs passively (and randomly), this number is impossible to reliably determine on a droplet-by-droplet basis, thus limiting the

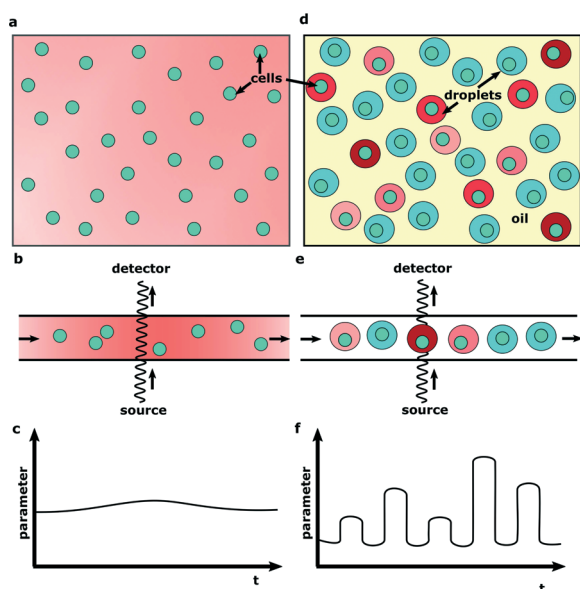


Fig. 1 Cell encapsulation enables efficient analysis of individual cells by confining them within a local microenvironment. (a–c) In conventional cell culture, ubiquitous fluid mixing only permits analysis of cells at the population level due to diffusive mixing of cellular products. (d) Encapsulation of cells within water-in-oil droplets prevents both advective and diffusive mixing. (e, f) Following encapsulation and incubation, parameters of interest can then be analyzed on an individual cell level in a high-throughput manner.

utility of passive cell encapsulation for single cell analysis.^{77,78}

To this end, recent research has explored more sophisticated microfluidic techniques to control the number of cells per droplet. Indeed, a number of these have shown substantial promise for dramatically improving the efficiency by which encapsulated single cells are produced. Furthermore, there are an increasing number of active methods available for droplet production and cell encapsulation, which are able to tune droplet size or produce droplets on-demand. Examples of active methods include those incorporating electrical, acoustic, optical and magnetic fields. These approaches have the advantage that they can be arbitrarily actuated and locally focused, and show substantial promise in addressing the deficits of purely hydrodynamic cell encapsulation. Surprisingly, previous reviews of cell-based analysis in microfluidic droplets have focused almost exclusively on hydrodynamic methods and/or emphasized the applications of encapsulated cells.^{9,37,62,75,76,79–81}

Moreover, although there are a plurality of methods for encapsulating cells, on both the micro and macro scales,⁷⁹ this analysis will focus specifically on microfluidic technologies used to encapsulate cells in two-phase systems, since these are better suited for en-masse, high-throughput and single-cell analysis applications. Additionally, because methods available for the encapsulation of cells are fundamentally those of droplet production, these methods are also discussed in the following sections, as future encapsulation methods are likely to be developed from the available suite of droplet production methods. These methods are also examined quantitatively in terms of their droplet production rate and potential to determine the number of cells per droplet beyond the limitations set by Poisson statistics.

2 Microfluidic droplet production

Although droplet production is ubiquitous in the microfluidic literature today, the microchannel geometries required to reliably create droplets were developed little more than a decade ago.^{83–86} Because of its ubiquity, one can be forgiven for forgetting how remarkable the process is; *i.e.* by exploiting a number of microfluidic geometries, a fluid of arbitrary volume can be transformed into a multitude of uniformly-sized femto-nanoliter droplets at rates of up to 100 kHz.⁸⁷ Moreover, given the length scale of the features used (typically between 10 and 100 μm) these channel designs can be duplicated on-chip for parallel processing. Common geometries for droplet production include T-junction, flow-focusing and co-flowing structures^{88,89} (Fig. 2), although variations on these themes have been reported, *e.g.* the V-junction or dual T-junctions.^{90,91} The underlying principle of operation for each of these geometries, however, is the same: an interface is created between two co-flowing immiscible fluids where one fluid self-segregates into discrete droplets that are surrounded by the second fluid. Which fluid becomes the dispersed phase (the one forming the droplets) and which

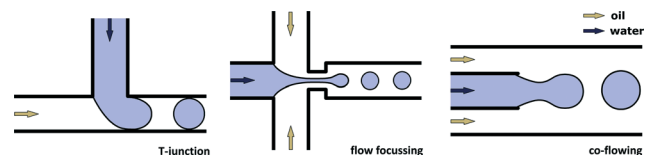


Fig. 2 Three principle microfluidic geometries are available for droplet production. In the simplest setup, oil and water are combined in a T-junction. Flow focusing and co-flowing geometries intersect the fluids in systems with both increasing degrees of symmetry and fabrication complexity from left to right, with bilateral and radial symmetry (if organized in a capillary-in-capillary setup)⁸² for co-flow and flow-focusing geometries, respectively.

forms the continuous phase (the one surrounding the droplets) is controlled by the respective surface energies of the fluid and that of the channel.⁹² In most cases, such as when using hydrophobic polydimethylsiloxane channels and oil/aqueous fluids, the aqueous phase disperses, although it is possible to initiate phase inversion through hydrophilic modification of the channel walls.⁹³

Droplet production processes are fundamental to the encapsulation of cells. Because of this, an understanding of the droplet-production toolkit is essential when selecting the particular method that should be employed in a given cell-encapsulation scenario. For fluidic self-segregation to occur, a pressure source that acts either on the fluid volume or the oil–water interface is required to push the dispersed phase into the continuous one. The next section explores the basic physics of fluid breakup into droplets and the different methods used to generate the required pressure gradients that give rise to this process.

2.1 Physics of droplet production

Despite the variety of methods used to drive the dispersed phase into the continuous one, the physics of droplet formation apply regardless. The physical parameters that dominate droplet formation can be determined through analysis of the capillary number $Ca = \mu U/\gamma$, where μ (Pa s) and U (m s^{-1}) are the viscosity and characteristic velocity of the continuous phase and γ (N m^{-1}) is the surface tension of the water–oil interface, although other non-dimensional quantities are relevant to droplet breakup, including the Weber number We (reporting the relative importance of inertia with respect to interfacial tension), Bond number Bo (reporting the relative importance of gravitational forces with respect to interfacial tension) and Reynolds number Re (reporting the relative importance of inertial forces with respect to viscous forces), especially at high flow rates and when using larger dimension geometries.⁹⁴ With increasing Ca , the different flow regimes are defined as the squeezing, dripping and jetting regimes.^{95,96}

In the surface-tension dominated squeezing regime, droplet pinch-off is driven by the pressure differential behind and in front of a confined extension of the fluid interface, where the resultant pinched-off droplet size is proportional to the

flow rate ratio of the dispersed and continuous phase. At higher Ca , droplet breakup and droplet size is shear-dominated (in the dripping regime) with a smaller pressure differential on either side of the nascent droplet than in the squeezing regime, yielding droplets whose size scales inversely with increasing Ca and with a reduced dependence on the flow rate ratio. Finally, in the jetting regime, droplet breakup occurs as a result of Rayleigh–Plateau instabilities along a fluid thread in viscosity-dominated flow. These three regimes are depicted in Fig. 3. For a more thorough discussion of these regimes and parameters that determine resultant droplet size, the reader is advised to peruse one of the excellent publications or reviews on the topic.^{94,95}

2.2 Passive droplet production

Droplet generation occurs passively if the pressure source is located remotely from the droplet formation geometry. Typically, the force driving fluid flow on-chip, as in Fig. 4a, is an externally driven pressure source, such as a syringe or pressure-driven pump. Because such macroscopic pressure sources are located at distances from the device that are orders of magnitude larger than the channel length scale, it is difficult (although not impossible) for the flow rates at the droplet forming geometry to be anything but continuous, thus resulting in continuous droplet production where the rate of individual droplets that are produced is a function of the fluid flow rates and the specific channel geometry and dimensions.⁷⁴ Examples of systems used to generate continuous streams of water-in-oil droplets have been covered extensively elsewhere.^{1,80,94} However, external pumps are not the only means by which pressure gradients can be produced for continuous droplet generation. For example, Häberle *et al.* demonstrated a method whereby a rotating microfluidic device is used to generate the centripetal force necessary to create droplets in a conventional flow-focusing geometry (Fig. 4b).⁹⁸

2.3 Active droplet production

There are other methods for producing pressure gradients, so that droplet production can occur on-demand with the application of an active, short-duration pressure source. As the timing, amplitude and duration of a pressure pulse can be

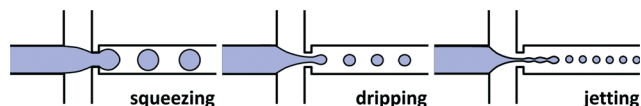


Fig. 3 Droplets are produced in the squeezing, dripping and jetting regimes with increasing capillary number, respectively. In the squeezing regime, the interface contacts both sides of the channel before breakoff. In the dripping regime droplet breakup is shear-dominated and the fluid interface is detached from the channel surface. At higher Ca (in the jetting regime) droplet breakup occurs due to Rayleigh–Plateau instabilities along an elongated fluid thread that extends into the outlet channel. In general, droplet size decreases with increasing Ca .

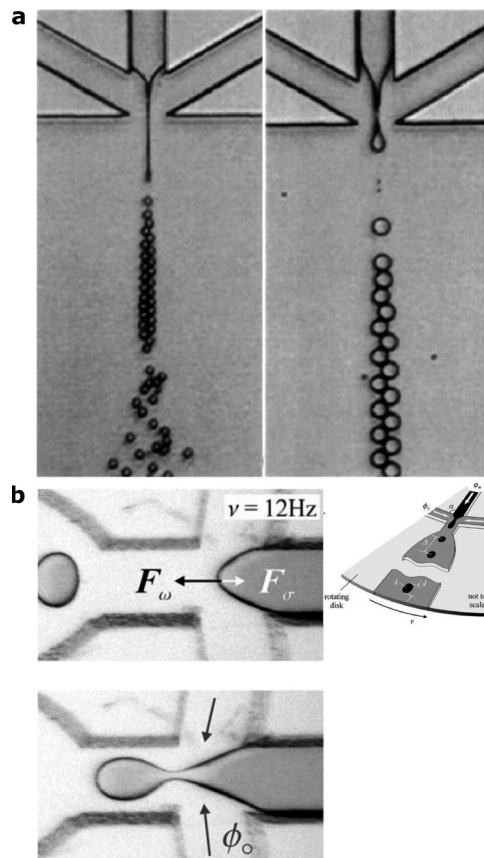


Fig. 4 (a) Droplets can be produced over a range of sizes by changing the ratio of oil and water flow rates, as controlled by external pressure sources. Reproduced with permission from ref. 97, copyright 2004, AIP Publishing. (b) Alternatives exist for generating continuous droplet streams, here showing a case where centripetal forces are used to drive fluid through a droplet-forming geometry. Reproduced with permission from ref. 98, copyright 2007, Springer.

arbitrarily set, such on-demand methods have the advantage of producing droplets of similarly arbitrary size and intervals. The most common active methods for droplet production are listed in Table 1. Park *et al.*, for example, used a focused pulsed laser to create a cavitating microbubble in the vicinity of a T-junction like structure, producing individual picoliter-volume water-in-oil droplets in the space of a few milliseconds and at rates up to 10 kHz (ref. 102) (Fig. 5d). Interestingly, this approach has also been used to produce femtoliter-volume droplets on-demand in nanofluidic channels.¹¹¹ In related work, Xu & Attinger utilized a piezoelectric actuator mounted on the chip surface, where each depression of the actuator produced an individual droplet.¹¹² However, while laser-induced cavitation or external actuation have the ability to produce droplets at kHz rates, such methods require complex external equipment to produce and focus laser pulses or substantial chip components that may be difficult to both scale down and reliably integrate. Recently, Collins *et al.* demonstrated the production of droplets using an on-chip pressure source arising from a focused surface acoustic wave (SAW), where conducting structures are patterned

Table 1 Comparison of active droplet production methods

Method	Production rate	Droplet volume (range)	Advantages/disadvantages	Mechanism	Ref.
On-demand production					
Focused surface acoustic wave (SAW)	<10 Hz	12–30 pL	On-chip control and combined particle manipulation, limited throughput	SAW is focused at a T-junction, changing pressure conditions at the oil–water interface.	101
Bimorph actuator	2.5 kHz	25 pL to 4.5 nL	High production rate and large size range, requires bonding of actuator	An actuator compresses a chamber, displacing fluid that is ejected into an oil-filled channel.	112
Pulsed laser excitation	10 kHz	1–150 pL	High production rate and large size range, requires equipment to drive on-chip cavitation	Laser-induced cavitation displaces fluid volume into an oil phase in a modified H-filter geometry.	102
Electrical potential	<50 Hz	14 fL to 8 pL	On-chip actuation, high voltages may not be compatible with biological samples	The leading edge of a water–oil interface is directed along an electric potential gradient.	99
Tunable rate					
Surface acoustic wave droplet rate modulation	~210–1100 Hz	~80–210 pL, ¹⁰³ ~30–140 pL (ref. 104)	Biocompatible method for continuously altering droplet size on-chip	Acoustic pressure is applied directly to an oil–water interface or to the continuous phase, with smaller droplets produced at higher powers.	103, 104
Electrical droplet rate modulation	10–500 Hz	~50–240 pL	Unknown effects of high voltage on biological samples	Electrical potential introduces maxwell pressure on interface, reducing droplet volume with increasing AC signals >600 V. For related work see ref. 118 and 105.	105
Pneumatic ‘chopping’	2–20 Hz, ¹²¹ ~2–40 Hz, ¹²² ~3.4–13.8 Hz (ref. 123)	~0.5–500 pL, ¹²¹ 100–1000 pL, ¹²² ~1–500 pL (ref. 123)	Biocompatible, requires integration of second bonded pneumatic layer	Pulsed pneumatic valve temporarily closes a microfluidic channel in a flow-focusing geometry, pinching off droplets with each pressure pulse.	121–123
Thermal viscosity change	Not given	100–300 pL	Chip-integrated strategy, temperature changes will effect biocompatibility	Local temperature changes up to 50 °C are induced using a microheater, changing local capillary number.	109
Optical modulation	O(1) Hz	Up to ~50% increase	Temperature changes will effect biocompatibility, requires optical toolkit	Laser is focused at the droplet formation region, where local heating temporarily blocks interfacial movement at the leading edge.	120
Thermomechanical valve	Not given	Up to ~50% decrease	Chip-integrated control, temperature changes will effect biocompatibility	Local heating causes channel deformations on the order of 1 μm, changing local capillary number.	107
Pneumatic geometry control	1.2–3.4 kHz	~1–125 pL	Biocompatible, requires integration of second bonded pneumatic layer	A flow-focusing channel outlet is constricted using pneumatic actuation, changing local capillary number.	106
Lab-on-a-disk	~20–400 Hz	~5–22 nL	Can be combined with other on-disk components, total volume limited by that on-disk	Droplets are created in a flow-focusing geometry by spinning the entire device, causing fluid flow from the central to outer regions.	98

directly on the piezoelectric device substrate¹⁰¹ (Fig. 5c). Other methods for creating local pressure sources include integrated micropumps^{100,113} and trans-interface electric-potential generation (Fig. 5a),⁹⁹ although it should be noted that these have yet to be directly applied to on-chip encapsulation.

Alternatively, as long as external pressure sources can be controlled with sufficient precision, they can also be used to produce droplets in an on-demand fashion. Integrated pneumatic microvalves can be used for this purpose (Fig. 5b),¹¹⁶ as can manually controlled microinjectors,¹¹⁷ though the rate at which the latter can accurately actuate the production of individual droplets is inherently limited by the capacitive and resistive effects of the channels and tubes through which the

pressure impulses are conducted. Aside from producing individual droplets, actively controlled forces can be used in conjunction with passive droplet production methods to alter the droplet size and production rate over shorter time scales than is possible using conventional pressure-driven sources alone.

Broadly, there are three ways the droplet volume can be tuned on-chip: applying a force at the fluid interface, changing fluid properties or altering channel dimensions. In an example of the first case, Schmid *et al.* used the interfacial acoustic pressure generated by a travelling acoustic wave to act both directly on the oil–water interface during droplet formation¹⁰³ and modulate the pressure in the continuous phase,¹⁰⁴ in both cases to tune the size of droplets produced

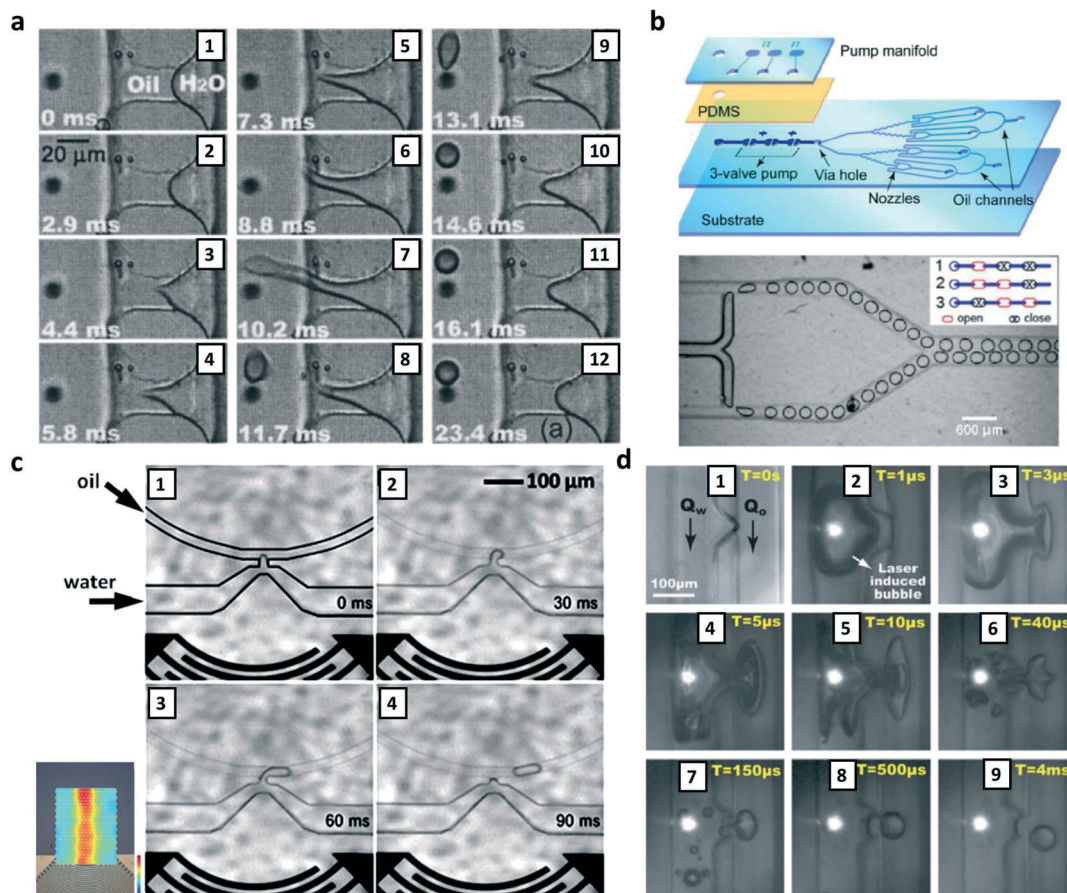


Fig. 5 A plurality of methods can be used to actively drive pressure gradients on-chip. Examples of these methods include (a) jet formation from an electrically generated Taylor cone, (b) the use of a pneumatically driven micropump, (c) acoustic force actuation and (d) laser-pulse excited cavitation. (a) Reproduced with permission from ref. 99, copyright 2005, AIP publishing. (b, c) Reproduced with permission from ref. 100 and 101, copyright 2013, The Royal Society of Chemistry. (d) Reproduced with permission from ref. 102, copyright 2011, The Royal Society of Chemistry.

continuously from an externally driven pressure source (Fig. 6a).

Interfacial forcing from an electrical source can similarly be used to modulate the size of continuously produced droplets. For example, Tan *et al.* used an electrical field to change the effective capillary number, with smaller droplets generated at higher AC voltages,¹⁰⁵ where the underlying mechanisms that determine the resultant droplet size are discussed in recent work.¹¹⁸ Optical sources can also be used to act on the fluid interface, where an optical beam is used to increase the residence time of a fluid–fluid interface prior to pinch-off, resulting in larger droplets for a higher applied power.^{119,120} The droplet volume can be similarly tuned by altering the fluid parameters, in effect altering the capillary number and thus the resultant droplet dimensions. For example, fluid in the vicinity of the droplet formation region can be heated, lowering the fluid viscosity and thus creating smaller droplets.^{108–110}

Finally, the channel dimensions can be modified in real-time. Here, volume tuning is achieved in one of two ways. The fluid can either be chopped, where the dispersed phase is segmented when a pneumatic pressure source is pulsed to temporarily close the channel, and where each pulse creates

a single droplet.^{121–123} Alternatively, the droplet forming region dimensions are constricted to increase the local fluid velocity, thus reducing droplet volume as a result of the increased capillary number (Fig. 6b).¹⁰⁶ In each of these examples, an external pneumatic source and an additional aligned elastomer layer containing air-filled channels is required, although Miralles *et al.* have reported the use of an integrated thermomechanical valve, where current flowing through a resistor heats and locally expands the PDMS channel at a T-junction, thus altering the size of droplets produced there.¹⁰⁷ However, given the relatively small deflections induced, the range of droplet sizes that can be produced is also small (see Table 1).

Given the limited work on active droplet production methods, it is not immediately apparent which approach is best suited to on-demand droplet production or applicable to cell encapsulation, though considerations including ease of fabrication, droplet production rate and general biocompatibility are all key parameters to be assessed. For on-demand generation, none of the demonstrated methods satisfy these criteria optimally; pulsed lasers and high-voltage electrical fields have questionable biocompatibility, while the acoustic and external actuation methods have demonstrated either

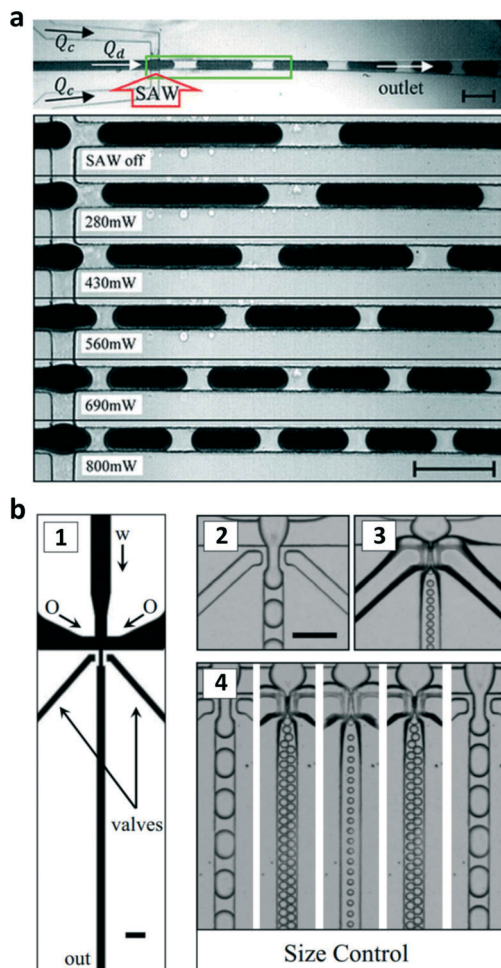


Fig. 6 Acoustic,^{103,104} electrical,¹⁰⁵ mechanical^{106,107} and thermal^{107–110} forces can be locally applied to actively tune the droplet dimensions and production rates. (a) Shows the use of a surface acoustic wave (SAW) to modify the local interfacial pressure conditions at the oil–water interface, promoting the generation of smaller droplets for increasing acoustic pressure. Reproduced with permission from ref. 103, copyright 2013, The Royal Society of Chemistry. In (b), integrated pneumatic valves are used to alter the droplet formation geometry, and thus local capillary number, to vary resultant droplet dimensions. Reproduced with permission from ref. 106, copyright 2009, AIP Publishing. All scale bars are 100 μm .

relatively slow generation rates or complex on-chip integration. However, the production rates listed in Table 1 are indicative only of the current state of development and do not represent inherent limits, as on-demand and novel droplet generation systems remain relatively under-developed. The same applies for active droplet size tuning methods, where the droplet production rate in principle should be able to equal or better than that of an equivalent passive droplet production platform, with the exception of pneumatically controlled flow chopping, which is fundamentally limited by the rate at which air-filled chambers can expand. With increasing development, miniaturization and implementation of on-chip actuation many of these on-demand active methods will be more frequently applied in applications

where precise control of the timing and rate of droplet formation is required.

3 Non-deterministic cell encapsulation

The bulk of published work in the area of cell encapsulation has used passive encapsulation methods to produce droplets whose occupancy is statistically determined. Although it is not possible to strictly determine the number of cells per droplet with these methods, the average number of cells per droplet can be controlled by changing the concentration of the incoming cell suspension. In addition to conventional passive encapsulation, several novel methods for the on-demand production of encapsulated cells have recently been demonstrated. These encapsulation methods are now presented, with methods for deterministically encapsulating cells (those that can specify the number of cells per droplet) discussed in the next section. Recently developed methods for non-deterministic cell encapsulation are compared in terms of their encapsulation rates in Table 2.

3.1 Passive encapsulation

A variety of cell encapsulation methods make use of either passively or actively formed droplets. Those methods using external pressure sources (syringe and pressure-driven pumps) comprise the bulk of work in the literature of cell encapsulation, including several reviews on encapsulation and single-cell analysis.^{62,79,80,124–127} Fig. 7a shows an example of passive encapsulation as typically applied, where the physics of encapsulation are tied to those of droplet formation, such that cells are encapsulated when they comprise a portion of the fluid volume that is segmented at the droplet-producing geometry. As the number of cells per droplet volume can significantly affect the viability of a particular process – the apparent reaction kinetics could double if two, rather than one, cell were encapsulated in a droplet, for example – it is strongly desirable to have a measure of control over this parameter. In the case where encapsulated cells are both numerous and significantly smaller than the droplets (such as with encapsulated micron-sized bacteria, for example),¹²⁸ the number of cells per droplet can reasonably be assumed to be representative of the volumetric concentration of cells.¹²⁹ However, for single-cell analysis this is not the case, where only one cell should be contained within the droplet volume. If cells are distributed randomly in an aqueous solution, the quantity of cells per encapsulated volume is determined by Poisson statistics. As the Poisson distribution either governs cell encapsulation rates in these systems, or is addressed through the addition of system features that attempt to circumvent it, the Poisson distribution is now discussed in detail.

For suspended cells traveling through microfluidic channels, the spatial distribution and therefore the timing of their arrival at the site of droplet formation is essentially random

Table 2 Representative non-deterministic on-demand and other novel encapsulation methods

Method	Encapsulation rate	Advantages/disadvantages	Mechanism	Ref.
On-demand methods				
Focused surface acoustic wave	<1 Hz	On-chip combined pre-concentration and droplet ejection mechanism, limited throughput	Acoustic pressure translates 10 μm particles to a water–oil interface prior to droplet formation.	101
Hydrodynamic bridges	<1 Hz	Simple to perform, limited throughput	Water droplet between two hydrophilic glass plates is expanded, forming an unstable fluid bridge that produces satellite droplets upon breakup.	115
Pulse-inertia	2–256 Hz	Effective single-cell encapsulation	An actuator expels individual droplets, some of which contain cells. Droplet size is tunable in order to maximize droplets containing a single cell.	130
Other methods				
Centrifuge	N/A	Simple method using common laboratory tools	A cell solution is forced through a nozzle at the base of a microtube insert in a lab centrifuge, producing momentarily airborne droplets that form hydrogel microbeads in a CaCl_2 solution. For related work see ref. 131.	132
Magnetic concentration	<30 Hz	Requires bound magnetically active particles	Magnetic field is used to pre-concentrate cells bound to magnetic particles prior to droplet formation.	133

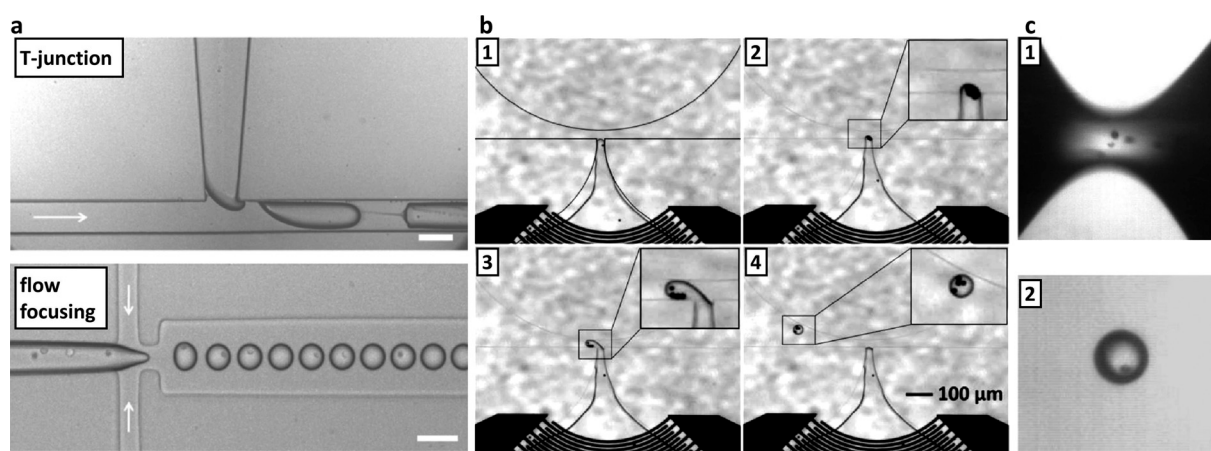


Fig. 7 There are a plurality of methods for encapsulating cells and particles in droplets. (a) In high-throughput applications, cells comprise a fraction of the aqueous volume that enters one of the droplet forming geometries presented in Fig. 2, where encapsulation occurs as a result of spontaneous droplet formation in fluids with different surface energies. Reproduced with permission from ref. 114, copyright 2010, IOP publishing. Alternative methods for encapsulation include concentration and ejection using (b) focused acoustic fields and (c) using hydrodynamically thinned fluid bridges. (b) Reproduced with permission from ref. 101, copyright 2013, The Royal Society of Chemistry. (c) Reproduced with permission from ref. 115, copyright 2014, Elsevier.

for passive encapsulation. For high cell concentrations and large droplets, the random distribution of cells is not a significant barrier to encapsulate an approximately equal number of cells per droplet, provided it is desirable that each droplet encapsulates a large number, where the number of cells in a droplet can be approximated by a Gaussian distribution. However, for applications requiring single-cell analysis, only one cell should be encapsulated per droplet. Here, the reaction products, cell signaling and metabolic output of each cell are fully contained, and thus independently measurable. The issue at the heart of producing a large number of encapsulated single cells is that if the arrival of cells at the water–oil interface is random while the production of droplets is continuous, there is no way to guarantee that a droplet will contain only a single cell, or even any cells at all.

Although cells arrive at the droplet formation region randomly, it is still possible to probabilistically estimate the proportion of single cells that are encapsulated according to the Poisson distribution, which is applicable in the case where the average cell arrival rate is known and the arrival of individual cells occurs independently from other cells. While the arrival rate is readily measurable (from the cell concentration in the feed solution), the second assumption does not strictly hold true, as two cells cannot inhabit the same volume. However, in the limiting case where the cellular volume fraction $\phi_s \ll 1$ (*i.e.* cells are sparsely distributed), where $\phi_s = \frac{\bar{Q}_c}{\bar{Q}_f}$, and \bar{Q}_c , \bar{Q}_f are the time-averaged volumetric flow rate of the cells and fluid flow rate, the assumption of independence is a valid one to make. Indeed, studies that have examined cell

encapsulation with a randomly distributed feedstock in this limiting case have shown good agreement with Poisson statistics. Finally, the Poisson distribution is given by

$$p(k, \lambda) = \frac{\lambda^k e^{-\lambda}}{k!}, \quad (1)$$

where k is the number of particles in a droplet and λ is the average number of cells per droplet volume. More thoroughly, λ can be defined as the ratio between the volume fraction of cells in the pre-encapsulation solution ϕ_s and that

of a droplet containing one cell, defined as $\phi_d \equiv \frac{\bar{V}_c}{\bar{V}_d}$, where

the average cell and droplet volume \bar{V}_c and \bar{V}_d are constant for given oil–water flow rates and system geometry. Thus, λ can also be expressed as

$$\lambda = \frac{\phi_s}{\phi_d}. \quad (2)$$

The Poisson distribution is examined in Fig. 8. As is often represented in the literature, Fig. 8a shows the Poisson distribution for different cellular concentrations as measured by λ . What can be inferred from this representation is that the average number of cells per droplet will rise for increasing cellular concentrations with a maximum number fraction centered on λ – the distribution eventually approximates a Gaussian distribution with mean and variance of λ (as $\lambda \rightarrow \infty$) – though for the range of cell concentrations used in single-cell encapsulation work ($\lambda < 1$), there is substantial variability in the number of cells that a given droplet might contain. A more useful representation of the distribution explicitly examines the proportion of droplets that contain a certain number of cells according to the parameter that the experimentalist can arbitrarily vary, *i.e.* λ . Solving $p(k, \lambda)$ for the proportion of droplets that contain one cell ($k = 1$) and the proportion of cell-containing droplets that contain exactly one ($k = 1 | k \geq 1$), Fig. 8b shows the operational cell concentration range for single-cell encapsulation. Here, the choice of cell concentration in the range $\lambda = (0, 1]$ depends on the capability of downstream sorting or measuring processes to detect the number of cells per droplet. Unsurprisingly, throughput of encapsulated single cells is maximized when $\lambda = 1$, where $1/e$ (~37%) of droplets contain single cells, though at the expense of specificity, with 42% of droplets containing more than one cell. Towards the lower limit of concentration (and cell throughput), for example at $\lambda = 0.05$, only 5% of droplets will have cell(s), though $k = 1$ for 98% of these. It should be emphasized, however, that regardless of λ , the majority of droplets will not contain single cells, requiring downstream sorting to produce an exclusively single-cell droplet emulsion. Having a sufficiently high percentage of single-cell droplets is an important factor, for example, in cell-pairing applications where two droplets containing individual cells are merged; in the case where $\lambda = 0.05$, only 0.25% of combined droplets will contain two cells if these droplets are merged at random.

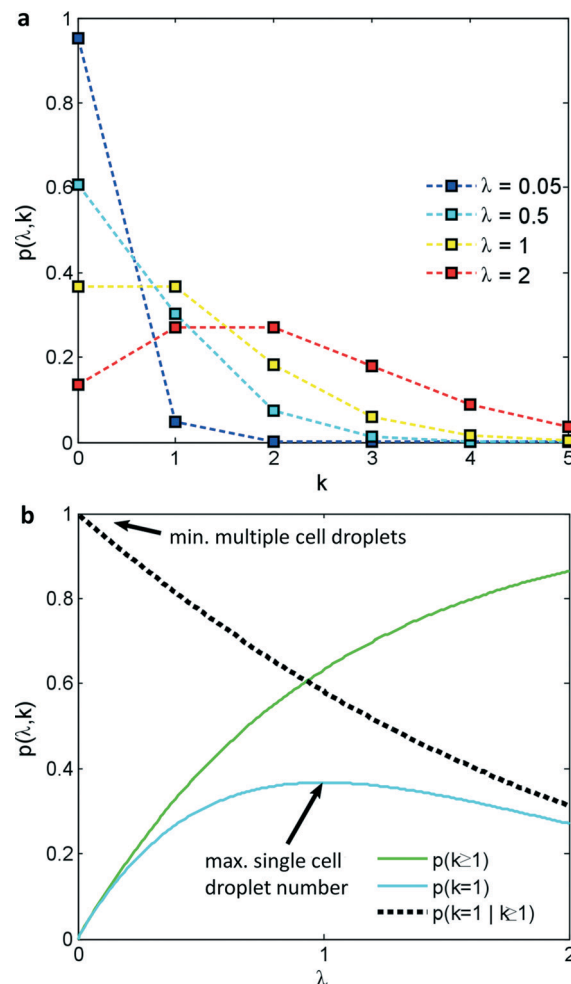


Fig. 8 The Poisson distribution is most commonly represented as in (a), where the proportion of droplets $p(\lambda, k)$ containing a given number of cells k is shown for different discrete values of λ . However, given that a defined number of cells per droplet are desired (most often one) for most applications, it makes sense to analyze the distribution according to the parameter that can be experimentally varied, λ , to determine the optimal cell concentration for given throughput and specificity requirements. (b) Shows the proportion of droplets that contain at least one cell, $p(k \geq 1)$, exactly one cell, $p(k=1)$, and the proportion of droplets containing cells that contain exactly one, $p(k=1 | k \geq 1)$. Single cell throughput is maximised when $\lambda = 1$, though at the cost of specificity, where only ~58% of droplets with cells and ~36% of all droplets will contain only one cell.

3.2 Active encapsulation

Given the nascent stage of active methods for droplet production, the predominance of passive encapsulation methods is somewhat justified, though there are several methods that show promise for improving aspects of the cell encapsulation process. Acoustic, electrical, optical or magnetic forces can be used to direct cells or particles to the droplet-producing region and actively create droplets when cells or particles approach the oil–water interface. Active methods for droplet production have the added advantage that the same forcing mechanism that is used to displace the oil–water interface to produce droplets also has the potential to act on solid–liquid

interfaces that direct cell motion in the vicinity of the interface. For example, Collins *et al.*, utilized a focused travelling SAW to both concentrate particles in solution at a water–oil interface and subsequently create a droplet encapsulating those particles (Fig. 7b)¹⁰¹ and to control the ejection of particles in a single phase.¹³⁴ In an alternative approach, Wang *et al.* fixed a piezoelectric actuator to the end of a glass capillary.¹³⁰ By pulsing the actuator, one or more droplets containing a number of cells could be ejected. Other novel methods for encapsulation include the formation of hydrodynamically-thinned bridges, which then segregate into droplets (some of which contain cells), as shown in Fig. 5c,¹¹⁵ the concentration and separation of magnetic particles in droplets,^{133,135,136} or the use of a centrifuge to eject and segment a cell-containing fluid from a glass capillary.¹³² These non-deterministic encapsulation methods are compared in Table 2.

As currently employed, however, the encapsulation rate using these methods is relatively limited. In contrast to passively formed droplets which can be formed at kHz rates, the encapsulation rate using most active techniques is orders of magnitude lower, even if the fact that only a fraction of passively produced droplets will contain single cells is taken into account. Optical positioning and subsequent encapsulation has been demonstrated at only sub-Hz frequency, for example.¹³⁷ For mass production of single-cell emulsions useful for high-throughput screening applications, encapsulation rates at least on the order of passively produced encapsulated droplets are required (>100 Hz), a production rate that is typical of high-throughput screening platforms.³⁹ Interestingly, active techniques have demonstrated phenomenal actuation rates in applications other than encapsulation. For example, Wu *et al.* were able to independently sort fluorescently-labelled lymphoma cells at rates of up to 20 kHz in a pure-aqueous media using pulsed-laser excitation.¹³⁸ Similarly, Franke *et al.* used a fluorescence-activated, localized SAW field to sort particles, cells and droplets at kHz rates.^{139,140} Active methods have yet to achieve similar rates for cell encapsulation, though the throughput in cell sorting achieved by active methods demonstrates the potential of active methods for this application. Given the high-speed actuation that is possible using these methods, it is expected that active techniques will soon be applied to the purpose of single-cell encapsulation in two-phase systems. Indeed, if recent patents are anything to go by, a system employing pulsed laser cavitation (in a similar setup to that in Wu *et al.*)¹³⁸ should demonstrate this in the near future.¹⁴¹

4 Deterministic single cell encapsulation

As discussed in Section 1, the random distribution of cells is a serious impediment to the efficient production of single-cell droplets. To circumvent the limitations posed by Poisson statistics, several approaches have been presented. These include the production of single cell emulsions by sorting

droplets after they have been passively created, inertial ordering of cells prior to encapsulation and on-demand cell encapsulation. Examples of these methodologies are summarized in Table 3. It should also be noted that another deterministic method has been demonstrated, where gel particles are closely packed prior to encapsulation so that they are released at a relatively constant rate.^{152,153} However, this method has limited applicability to cells, which are far more likely to block channels if their concentration is too high.

4.1 Single-cell emulsions by sorting

One route to obtaining high purity single-cell emulsions is to separate encapsulated cells from a stream of droplets, the vast majority of which are empty (in the case where $\lambda \ll 1$). Post-encapsulation sorting draws on the large body of work in cell, particle and droplet sorting, where cells can be sorted according to their physical dimensions, electromagnetic susceptibility, or mechanical and optical properties. Active sorting approaches, including those demonstrated in single-phase systems, make use of acoustic fields,^{139,140,154–158} optical forces,^{159–161} and electric fields,^{154,162,163} or purely hydrodynamic ones such as deterministic lateral displacement (DLD),^{144,164} shear-induced migration¹⁴⁷ and inertial microfluidics in spiral microchannels.¹⁶⁵ Many of these same hydrodynamic and active mechanisms have been utilized for high-frequency single-cell droplet sorting applied downstream of the droplet generation zone, though it is conceivable that any of them could be applied for this purpose. Active methods offer the most flexibility in sorting droplets, where any measurable quantity can be used for sorting. Using a continuously applied standing wave acoustic field, Nam *et al.* were successful in sorting alginate droplets according to the number of cells contained, where those with more cells migrate more rapidly to a standing wave nodal position by virtue of their marginally greater density and subsequent acoustic contrast factor¹⁴³ (Fig. 9a). Importantly, employing such a mechanism opens up the possibility of sorting droplets based on the quantity of cells that they contain, and not just the presence or absence of cells. On-demand sorting methods such as those using localized fluorescence-activated dielectrophoretic (DEP) forces can further expand the versatility of cell sorting to include a measure of cell function. For example, Agresti *et al.* used a DEP-based sorting device to separate droplets (containing cells) expressing a threshold level of horseradish peroxidase⁶⁵ (Fig. 9b). Localized acoustic fields have also been used for the sorting of cells and droplets,¹⁶⁶ at rates of up to 3 kHz.¹⁴⁰ Other excellent examples of microfluidic fluorescence-activated cell sorting have been reported.^{54,142,167–169}

The addition of a fluorescent or chemical reporter can increase sensitivity to the detection of cells and their function,^{170–173} however label-free detection is also feasible, permitting the high-speed analysis of cells without the requirement for added reporters. These on-chip detection methods, including optical and electrical ones, are covered in

Table 3 Deterministic methods for single-cell encapsulation

Method	Droplet sorting/production rate (Hz)	Encapsulated cell(s) rate (Hz)	Efficiency (%)	Advantages/disadvantages	Mechanism	Ref.
Post-encapsulation sorting						
Dielectrophoresis FACS	~2 kHz	~0.4 kHz (single cells)	>99% sorting efficiency	Rapid sorting, requires optical sensing apparatus	Dielectrophoretic force directs optically analyzed droplets into a separate outlet. For related work see ref. 39 and 68.	65, 142
Travelling acoustic wave FACS	3 kHz	<3 kHz	Not provided, near 100% sorting presumed	Rapid sorting, requires optical sensing apparatus	Acoustic force/streaming directs optically detected cells into a separate outlet. For related work see ref. 139.	140
Standing acoustic wave continuous	~40 Hz	<40 Hz	97% of desired cell density beads separated	No sensing equipment required, sort on non-size parameter	Beads containing different numbers of cells exhibit differential migration in an acoustic field by virtue of their different average densities.	143
Deterministic lateral displacement	5 kHz	~2–200 Hz	~60–78% of sorted droplets contain single cells	Passive sorting, requires large chip area for DLD array	Droplets containing cells are larger, and therefore sorted from empty droplets in a DLD array. For an explanation of DLD principles, see ref. 144, and for related work see ref. 145.	146
Shear migration	Not provided	20–160 Hz	96 ± 3% of sorted contain single cells, 20–30% false negative (typical)	Passive sorting, optimized flow rates required	Cells initiate the formation of larger droplets in the jetting regime, which are then sorted from empty droplets <i>via</i> differential shear-induced migration rates.	147
Pinched flow fractionation	<200 Hz	Not provided	~50% of sorted contain single cells	Passive sorting, though low flow rates on the order of $\mu\text{L h}^{-1}$ used	A large droplet containing multiple cells is broken up into smaller droplets using a microgroove structure, with smaller (empty) droplets separated from larger, cell-containing ones <i>via</i> pinched-flow fractionation.	148
Inertial ordering						
Straight microchannel	14.9 kHz	12 kHz	~80% contain single cells	Rapid throughput, tuned flow rates and concentrations required	Evenly-spaced cells arrive at a droplet generating geometry at a similar rate to that of droplet production due to inertial ordering.	149
Dean-flow microchannel	2.7 kHz	~2.2 kHz	~80% contain single cells	Rapid throughput, tuned flow rates and concentrations required	Similar to straight-microchannel ordering, except Dean flow biases collection into a single focused line. For related work see ref. 33.	150
Active detection and encapsulation						
Cell sensing and pico-ejection	<1 Hz	<1 Hz	73 ± 11% of single cells are ejected	Active single-cell droplet ejection with potential for throughput, low rate demonstrated	Suspended cells in flow are sensed using a local impedance measurement, whereafter they are dispensed with individual depressions of a piezoelectric actuator.	151
Optical trapping	<1 Hz	<1 Hz	100% of translated cells ejected	High cell selectivity, requires operator with low potential for throughput	Cells or sub-cellular components are brought to the oil–water interface using optical tweezers prior to droplet formation.	137

a recent review article.¹⁷⁴ Though many have not yet been utilized in conjunction with post-encapsulation sorting, it is worthwhile discussing detection methods that could be in future work. Kemna *et al.*, for example, were able to detect 80% of encapsulated cells at >100 Hz by measuring the difference in electrical impedance between a droplet with and without a cell that passes above a set of parallel electrodes;¹⁷⁵

the addition of an active sorting system post-cell detection could be a viable method for the production of single cell droplets. Mass spectrometry, while requiring the requisite equipment, has the ability to measure fine-grained information about cells and their local environment.¹⁷⁶ Shigeta *et al.* were able to detect femtogram amounts of trace elements (selenium, zinc, *etc.*) in yeast cells at 50 Hz rates using inductively

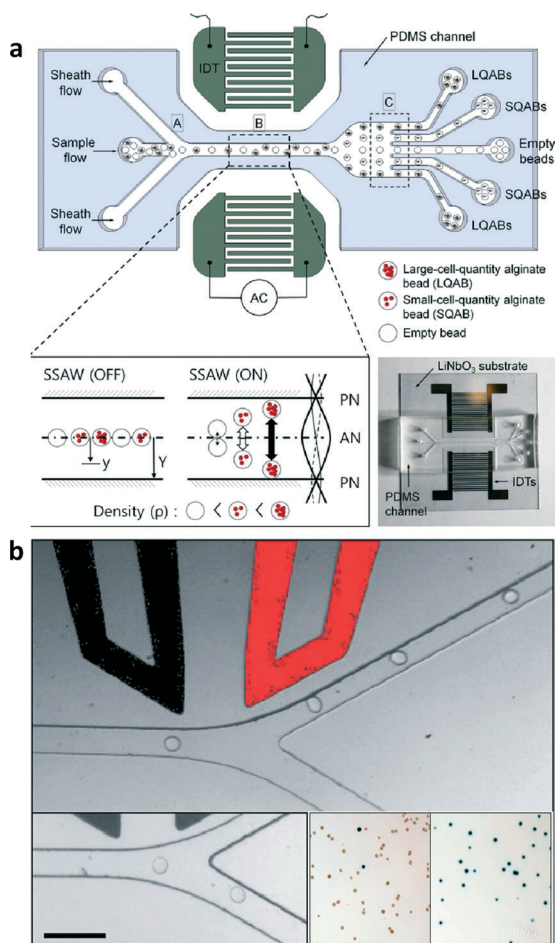


Fig. 9 Actively applied forces can be used to sort droplets on parameters other than their dimensions. (a) Using a standing SAW field, Nam *et al.* continuously sorted alginate hydrogel beads according to the number of cells contained. Reproduced with permission from ref. 143 copyright 2012, AIP publishing. (b) Localized DEP can sort individual droplets according to a measured property such as fluorescence or other optically measured parameters; upper image shows droplets being actively directed upwards or passively allowed downwards (lower left), where the set of images in the lower right shows the plated cell cultures from unenriched (left) and enriched (right) droplet populations. Scale bar is 100 μm . Reproduced with permission from ref. 142, copyright 2009, Royal Society of Chemistry.

coupled plasma mass spectrometry (ICP-MS),²⁰³ useful for the detection of metals, and similar to work by Smith *et al.* where protein concentrations were detected in droplets at 150 Hz using electrospray ionization mass spectrometry (ESI-MS).¹⁷⁷ However, the need to create an aerosol prior to detection – mass spectrometry requires the input of sample ions in the gas phase – with these two methods precludes the use of a two-phase system wherein cells can be encapsulated pre-aerosol formation. Küster *et al.* avoids the need to create an aerosol while making use of two-phase encapsulated cells by first depositing them on a surface-treated substrate to trap individual droplets, whereupon mass spectrometry is performed on a droplet-by-droplet basis after the evaporation of the aqueous and volatile oil phases.²⁰⁴ Direct optical detection is more readily integrated into microfluidic systems,

given the transparent nature of the materials typically used (glass, PDMS, PMMA, *etc.*), which permits in-line analysis to increasingly refined levels; Yu *et al.* demonstrated the detection of 10 nm-scale bacteriophages in droplets containing *Escherichia coli* via optical scattering.¹²⁸ In a label-free analogue to the work from ref. 39, 65, 68 and 142, Zang *et al.* integrated high speed optical detection to perform growth-dependent enrichment of encapsulated bacteria using electrical sorting at >100 Hz.¹⁷⁸

Hydrodynamic methods can be used to sort droplets on the basis of their size, where the presence of a cell in a droplet alters its dimensions. In one avenue for producing differently-sized droplets in this manner, a cell in a thinning capillary thread (produced in the jetting regime) serves as an early nucleation site for Rayleigh-plateau instabilities, resulting in the production of droplets larger than those that do not contain cells (Fig. 10b-1). Chabert & Viovy demonstrated post-encapsulation sorting *via* shear-induced migration of larger droplets to the channel center and a form of pinched-flow fractionation (PFF)¹⁴⁷ (Fig. 10a), a sorting method used similarly by Um *et al.*, though to a lower single cell enrichment level¹⁴⁸ (see Table 3). Alternatively, Jing *et al.* made use of a DLD pillar array for post-encapsulation sorting, where larger droplets containing cells were translated at an angle to the flow, and thus sorted from the smaller empty droplets (Fig. 8b).¹⁴⁶ While encapsulating in the jetting regime has the advantage of pre-ordering cells in the thin fluid thread, a shortcoming of such an approach is that the resultant droplet dimensions are limited to volumes on the order of cells if the size difference is to be sufficient for hydrodynamic sorting. There is, however, at least one other avenue for inducing cell-dependent droplet size differences. Joensson *et al.* were able to shrink droplets containing yeast cells *via* osmosis in an lipophilic phase in which water is partially soluble, where after the cell-containing droplets were sorted using DLD.¹⁴⁵ Though other methods of size-based droplet sorting have been reported, including the use of size-selective patterned tracks^{179,180} and a differential fluid shear mechanism,¹⁸¹ DLD and PFF sorting methods present the best opportunity for high-throughput purely hydrodynamic post-encapsulation cell sorting.

Active methods as employed have improved sorting efficiency and speed compared to passive methods, as noted in Table 3. Baret *et al.*, for example, were able to sort individual droplets at rates up to 2 kHz with error rates of 0.01–1%,¹⁴² comparing favourably with false positive and negative rates of approximately 4% and 20%, respectively, in the shear-induced migration sorting reported by Chabert *et al.*¹⁴⁷ Active sorting also permits the detection of not only the presence of cells, but also of cell properties, which when combined with a low error rate is especially important in applications involving rare cells. Efficiently performed directed evolution, for example, requires that mutations in a small proportion of cells can be positively selected for; active forces are used here as their activation can be coupled with the optical detection of desired cell traits. Active post-encapsulation cell sorting

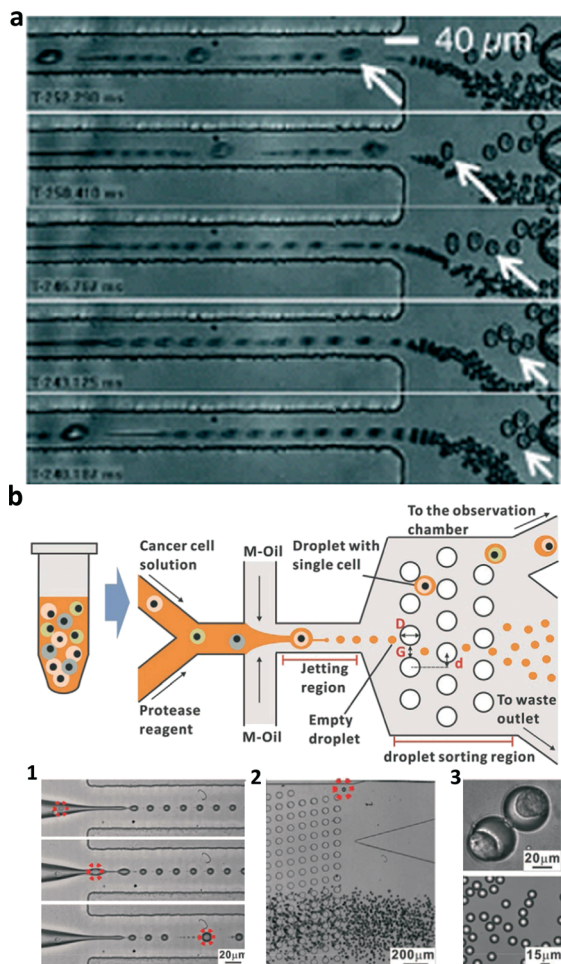


Fig. 10 Passive post-encapsulation sorting methods separate encapsulated cells from empty droplets based on the substantial size differences between the two. If produced in the jetting regime, where the width of the fluid thread is on the order of the cell dimensions, larger droplets containing cells can be sorted from the empty ones using (a) shear-induced migration and pinched-flow fractionation (PFF) or (b) mechanical-pillar deterministic lateral displacement (DLD). (b-1) In both (a) and (b), larger cell-containing droplets are produced when a cell serves as a nucleation site for Rayleigh–Plateau instabilities in the jetting regime. (b-2) shows the separation of numerous small droplets from cell-containing droplets (circled in red) in a DLD array, while (b-3) shows the substantial size differences in the sorted cell containing (top) and empty (bottom) droplets. (a) Reproduced with permission from ref. 147, copyright 2008, National Academy of Sciences. (b) Reproduced with permission from ref. 146, copyright 2015, Elsevier.

devices can also make use of entirely separate droplet formation geometries that can tune the droplet size to a wide range of volumes – potentially on an entirely different device – without the need to couple flow rates and droplet volumes between droplet generation and sorting functions. On the other hand, improved sorting fidelity and flexibility comes at the cost of increased device complexity, where multiple structures need to be aligned, calibrated and driven by external equipment.

4.2 Inertial cell ordering

Though sorting methods have the demonstrated ability to produce high-purity single cell emulsions, their throughput

is fundamentally limited by the rate at which single cells are initially encapsulated, which itself is determined by Poisson statistics. For typical cell concentrations ($0.01 \lesssim \lambda \lesssim 0.1$), only a few percent of droplets that are produced will contain cells, with the sorted empty droplets volumes being wasted. While this waste is more often than not a secondary concern, where the total volume of wasted picoliter scale droplets might be on the order of microliters, the aggregate time spent producing them in a given droplet geometry reduces the maximum throughput by at least an order of magnitude.

A sensible solution to increase throughput is to employ a method whereby each droplet that is produced contains a single cell; if cells arrive at the formation geometry at the same rate that droplets are produced, every droplet will contain one cell. To this end, Edd *et al.* demonstrated a method they termed inertial ordering to focus particles and cells at defined positions both laterally and longitudinally in a rectangular channel prior to droplet formation (Fig. 11a).¹⁴⁹ Stable particle positions are produced laterally where the force resulting from the parabolic-profile shear gradient (pushing particles to the channel edges) is balanced by that of the wall interaction force,^{124–126} the latter analogous to the ground effect utilized by some aircraft.¹⁸² Longitudinally, particles are ordered by what has been termed a hydrodynamic repulsion effect resulting from inter-particle interactions.^{127,183–185}

It has been demonstrated that this hydrodynamic effect is a result of reversing fluid streamlines in the vicinity of a rotating particle, repelling nearby particles.¹⁸⁵ Interestingly, this repelling effect can be manipulated, where the distance between neighboring particles is a function of the channel width,¹⁸⁶ though as channel dimensions are difficult to modify *in situ*, the encapsulation rate must be controlled by fine-tuning of the input flow rates.

Although Edd and co-workers produced staggered particles and cells on either side of a channel, it is also possible to focus these particles into a single line. By introducing asymmetric curve(s) in the channel geometry a secondary Dean flow is produced that reduces the number of stable equilibrium positions. A commonly employed method to produce this asymmetry and therefore inertial focusing makes use of curved channels.¹⁸³ Kemna *et al.* and Schoeman *et al.* demonstrated lateral focusing and longitudinal ordering in spiral microchannels, where cells were similarly encapsulated such that the majority of droplets produced contain single cells^{33,150} (Fig. 9b). An advantage of inertial ordering is that individual cells can be encapsulated at throughputs orders of magnitude more than without ordering. Indeed, in the studies by Edd, Kemna and Schoeman the cell concentration can approach the theoretical maximum single-cell output with input concentrations near $\lambda = 1$. Furthermore, being able to encapsulate cells deterministically permits activities that would be impractical without pre-ordering. Lagus & Edd and Schoeman *et al.* were able to demonstrate cell-pair co-encapsulation using two separate ordered-cell inlets that intersect at a flow-focusing geometry,^{33,187} without pre-ordering the proportion of droplets that contain one of each particle or

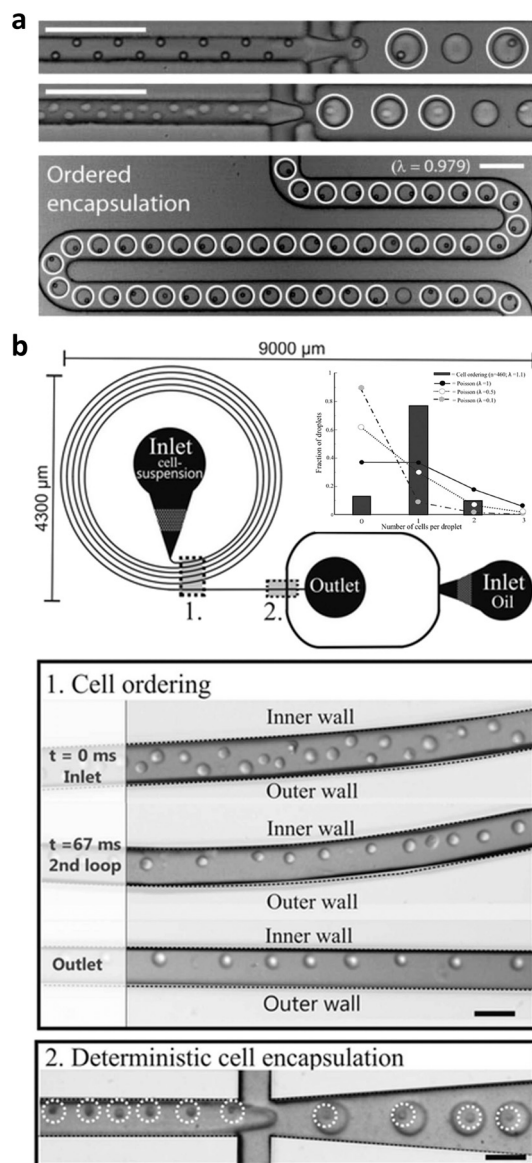


Fig. 11 Inertial ordering has the potential to drastically increase the proportion of droplets produced that contain single cells. Using (a) straight or (b) curved microchannels at suitable Reynolds numbers, particles can be focused at discrete locations laterally and ordered longitudinally. Both inertial ordering systems demonstrate significant improvement in single-cell capture efficiency as compared to what might be expected of randomly arriving cells or particles (top right of (b)). (a) Reproduced with permission from ref. 149, copyright 2008, Royal Society of Chemistry. (b) Reproduced with permission from ref. 150, copyright 2012, Royal Society of Chemistry. Scale bars denote (a) 100 μm and (b) 50 μm .

cell would be significantly lower. Despite the advantages conferred by inertial ordering for single-cell encapsulation, in practice this method can be difficult to implement, especially for a cell population with heterogeneous characteristics. Moreover, for one cell to be encapsulated per droplet, the rate at which cells arrive at the droplet forming geometry must be equal to the rate of droplet formation, requiring finely balanced flow rates for aqueous and oil inflows.

Finally, inertial ordering requires flow rates higher than typically used in microfluidic systems, with $1 < \text{Re} < 300$ and flow velocities on the order of $\sim 0.1\text{--}1 \text{ m s}^{-1}$, limiting the range of other microfluidic processes this method can be coupled with.

4.3 On-demand encapsulation

An emerging methodology for the encapsulation of single cells combines the detection of cells in a constant flow with the ability to produce droplets on-demand. In this methodology, single cell droplets are produced when an automated system detects the presence of a cell and triggers the production of a droplet. This differs from the case demonstrated a decade ago, where optical trapping was used to guide an individual cell to the fluid–fluid interface, a methodology that is not inherently suited to even moderate-throughput applications.¹³⁷ Though to date this detection and ejection methodology has been developed only for water–air phase systems, it could be equally successful in a water–oil one; this phase combination could be effectively obtained by ejecting droplets through air into an oil reservoir. In an example of single-cell printing, Schoendube *et al.* used a set of electrodes to detect the local electrical impedance change induced by the presence of a cell in a continuous flow, ejecting a single cell when it arrived at the dispensing port.¹⁵¹ Here, a piezoelectric actuator was pulsed after a delay period corresponding to the flow rate in the cell channel to eject a single droplet containing the detected cell. Automated optical detection permits the same activity, though in those cases demonstrated droplets are produced continuously, where waste droplets are ejected into a separate reservoir.¹⁸⁹ Leibacher *et al.* and Gross *et al.* made use of a shuttered vacuum source to sort waste droplets, where Leibacher *et al.* further refined the system using an acoustic standing wave to align cells prior to ejection, thus increasing detection and therefore encapsulation efficiencies.^{188,190} Fig. 12 shows the geometries of the single-cell printing systems utilized in these studies.

5 Recent applications

The value of encapsulated cells is reflected in the wide range of applications where they have been used. This includes recent applications in diagnostics and therapeutics, which are briefly discussed here. A growing area for the use of encapsulated cells is in tissue engineering, where cells are encapsulated in a hydrogel matrix that effectively serves as an extracellular matrix.¹⁹¹ Bulk hydrogel-cell composites have been used extensively for *in vivo* tissue generation, for example being used to assist in neural regeneration after injury.¹⁹² However, there is growing recognition of the value in encapsulating cells in discrete quantities, in individual hydrogel droplets rather than en-masse, permitting the preparation of non-homogeneous engineered tissues. Here, cells are encapsulated in an almost identical process to oil–water systems, except that by using a photo- or chemo-catalyzed hydrogel the bead can be stably suspended in an aqueous

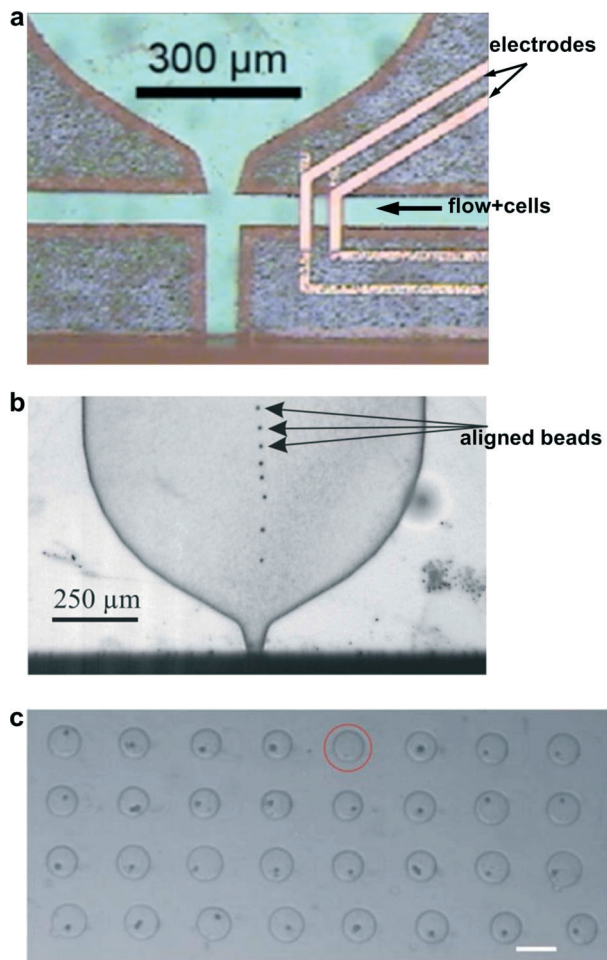


Fig. 12 Active single-cell encapsulation has been demonstrated in a limited number of cases, where detection methods are used to determine the presence of cells. In (a), the passage and velocity of a cell is measured in real-time, triggering the ejection of a single encapsulated cell after a delay. Reproduced with permission from ref. 151, copyright 2015, AIP publishing. (b) Automated optical detection is also possible, and when combined with a method for aligning particles or cells, can improve the encapsulation efficiency. Reproduced with permission from ref. 188, copyright 2015, AIP publishing. (c) Using these systems, single-cells can be ejected into microwell arrays. Scale bar is 200 μm. Reproduced with permission from ref. 189, copyright 2011, Royal Society of Chemistry.

phase.^{79,193–195} For example, Lin *et al.* used optical forces to direct the positions of alginate beads containing different densities of chondrocytes in order to mimic the spatial gradient of these cells in articular cartilage.¹⁹⁶ Other benefits of encapsulating cells include improving the surface area-to-volume characteristics for nutrient diffusion, preventing or mediating the immune response to cells and maintaining pluripotency of stem cell culture.^{197,198} Interestingly, encapsulation also allows cells to be used effectively as therapeutic agents in their own right, where encapsulated cells hold substantial promise for delivery of cell-produced drugs. Here, a (potentially engineered) cell is used to emit the desired biopharmaceutical, where local nutrients are used to produce the drug on-site and where resulting metabolites can freely

diffuse through the hydrogel matrix surrounding the cell(s). These benefits are further enhanced in a core-shell capsule, where a hydrogel bead is encased in a secondary polymer shell to prevent ingress or egress of cells.¹⁹⁹ For a thorough discussion of many of these applications, the reader is advised to view an excellent review on the topic.⁶¹

Encapsulated cells are uniquely suited to applications in high-throughput screening, which leverages the ability to produce, screen and sort droplets in microfluidic systems at kHz rates to select for desired cell characteristics, often mediated by a fluorescent reporter. Distinguishing this from single-phase FACS, encapsulation enables the long-term incubation of cells in a unique microenvironment so that cells can be individually assessed on their exogenous products rather than only endogenous ones. It is then unsurprising that encapsulated cells have especially found application in the screening and enrichment of enzymes produced by cells; screening and selection of cells that produce these enzymes can be used to improve their properties, important as enzymes are widely used in commercial applications.²⁰⁰ For example, Ostafe *et al.* used two separate microfluidic devices one to encapsulate and a separate one to sort in order to select for cells expressing high cellulase activity, demonstrating a 300-fold enrichment over a single pass.¹⁶⁸ This scheme can also be performed over several passes, where cells selected from one population are used to generate offspring for subsequently screened generations, in a process justly termed directed evolution. This has been used to vastly improve the enzymatic activity of horseradish peroxidase through the evolution of mutants⁶⁵ and enrich the quantity of transformed bacteria.²⁰¹ Sjostrom *et al.* took the further step of, rather than relying on natural mutation rates and variations in activity, creating a library of UV-mutated yeast prior to sorting.¹⁷ A potential drawback of constant throughput screening is the inability to track the life cycle of individual cells over multiple passes. However, it is not necessary to have encapsulated cells move to assay their activity. Shemesh *et al.* encapsulated individual cells *in situ* to observe their metabolic activity over several hours.²⁰²

6 Summary and prospects

A number of droplet production methods for the purpose of microfluidic encapsulation have been presented and discussed. As is often the case in engineering enterprises, the particular method best suited for a given application is a function of the operational parameters of that application, though naturally only methods that have reached a sufficient level of development can be considered. To date, the majority of studies employing cell encapsulation and single-cell analysis have utilized passive encapsulation methods using pressure-driven flow in droplet forming geometries, where droplet production can occur on the order of kHz. However, despite this impressive throughput, Poisson statistics fundamentally limit the rate at which a reliable number of cells can be encapsulated. Up to a point, higher input cell

concentrations will increase single-cell throughput, though at most only 37% of droplets will contain only one cell, and therefore at least 67% of droplets are either wasted and/or require removal, with the result that the maximum throughput of encapsulated cells is an order of magnitude lower than the droplet production rate.

Inertial ordering methods have demonstrated the ability to vastly improve single-cell encapsulation efficiencies up to 80%, although they are limited in their range of applications due to practical constraints; high flow rates and specific cell concentrations are required to achieve the longitudinal ordering needed. These constraints strongly restrict the types of systems that this droplet production method can be directly integrated with. Additionally, even pre-ordering of cells prior to encapsulation will leave a substantial proportion of droplets that do not contain the requisite number of cells, which may be undesirable for many applications. Passive methods have been developed for post-encapsulation sorting based on size, but they too leave a substantial proportion of droplets that are either unsorted or wrongly allocated. Similarly, for applications the cell waste resulting from lossy sorting methods may be unacceptable.

On the other hand, active sorting methods have demonstrated the ability to sort droplets according to their contents with near 100% fidelity, and can be applied for parameters other than size, including cellular activity and cell number, with sorting rates up to 10 kHz. Furthermore, though less developed for this application, active methods have the potential to address many of the shortcomings of passive droplet production and encapsulation systems. With these methods, forces are generated near fluid–fluid interfaces for on-demand droplet production, with similarly high droplet production rates realized in some systems. When coupled with systems to detect the presence of cells, these methods will have the ability to similarly encapsulate droplets on-demand to directly produce near-perfect single-cell emulsions without the need for downstream sorting. Though a truly high-throughput on-demand single-cell encapsulation system has yet to be realized, it is expected that the future development of these active methods will substantially improve the performance of applications where encapsulated single-cells are required.

Acknowledgements

The material reported in this document is supported by the SUTD-MIT International Design Centre (IDC). Any findings, conclusions, recommendations, or opinions expressed in this document are those of the author(s) and do not necessarily reflect the views of the IDC.

References

- 1 H. A. Stone, A. D. Stroock and A. Ajdari, *Annu. Rev. Fluid Mech.*, 2004, **36**, 381–411.
- 2 K. Ino, M. Okochi, N. Konishi, M. Nakatochi, R. Imai, M. Shikida, A. Ito and H. Honda, *Lab Chip*, 2008, **8**, 134–142.
- 3 S. Haeberle and R. Zengerle, *Lab Chip*, 2007, **7**, 1094–1110.
- 4 H. Shafiee, S. Wang, F. Inci, M. Toy, T. J. Henrich, D. R. Kuritzkes and U. Demirci, *Annu. Rev. Med.*, 2015, **66**, 387–405.
- 5 S.-B. Huang, M.-H. Wu, Y.-H. Lin, C.-H. Hsieh, C.-L. Yang, H.-C. Lin, C.-P. Tseng and G.-B. Lee, *Lab Chip*, 2013, **13**, 1371–1383.
- 6 P. Neuži, S. Giselbrecht, K. Länge, T. J. Huang and A. Manz, *Nat. Rev. Drug Discovery*, 2012, **11**, 620–632.
- 7 S. N. Bhatia and D. E. Ingber, *Nat. Biotechnol.*, 2014, **32**, 760–772.
- 8 R. Jiang, M. J. Jones, E. Chen, S. M. Neumann, H. B. Fraser, G. E. Miller and M. S. Kobor, *Sci. Rep.*, 2015, **5**, 8257.
- 9 D. Wang and S. Bodovitz, *Trends Biotechnol.*, 2010, **28**, 281–290.
- 10 G. T. Roman, Y. Chen, P. Viberg, A. H. Culbertson and C. T. Culbertson, *Anal. Bioanal. Chem.*, 2007, **387**, 9–12.
- 11 H. Yin and D. Marshall, *Curr. Opin. Biotechnol.*, 2012, **23**, 110–119.
- 12 S. Lindström and H. Andersson-Svahn, *Lab Chip*, 2010, **10**, 3363–3372.
- 13 R. P. Kulkarni, J. Che, M. Dhar and D. Di Carlo, *Lab Chip*, 2014, **14**, 3663–3667.
- 14 V. Lecault, A. K. White, A. Singhal and C. L. Hansen, *Curr. Opin. Chem. Biol.*, 2012, **16**, 381–390.
- 15 C. J. Ye, J. B. Stevens, G. Liu, S. W. Bremer, A. S. Jaiswal, K. J. Ye, M.-F. Lin, L. Lawrenson, W. D. Lancaster, M. Kurkinen, J. D. Liao, C. G. Gairola, M. P. Shekhar, S. Narayan, F. R. Miller and H. H. Heng, *J. Cell. Physiol.*, 2009, **219**, 288–300.
- 16 A. Y. Fu, C. Spence, A. Scherer, F. H. Arnold and S. R. Quake, *Nat. Biotechnol.*, 1999, **17**, 1109–1111.
- 17 S. L. Sjöstrom, Y. Bai, M. Huang, Z. Liu, J. Nielsen, H. N. Joensson and H. A. Svahn, *Lab Chip*, 2014, **14**, 806–813.
- 18 X. Niu, F. Gielen, J. B. Edel and A. J. deMello, *Nat. Chem.*, 2011, **3**, 437–442.
- 19 O. D. Laerum and T. Farsund, *Cytometry*, 1981, **2**, 1–13.
- 20 W. Bonner, H. Hulet, R. Sweet and L. Herzenberg, *Rev. Sci. Instrum.*, 1972, **43**, 404–409.
- 21 H. E. Ayliffe, A. Bruno Frazier and R. Rabbitt, *J. Microelectromech. Syst.*, 1999, **8**, 50–57.
- 22 O. Saleh and L. Sohn, *Rev. Sci. Instrum.*, 2001, **72**, 4449–4451.
- 23 S. J. Tan, M. Z. Kee, A. S. Mathuru, W. F. Burkholder and S. J. Jesuthasan, *PLoS One*, 2013, **8**, e78261.
- 24 S. J. Tan, H. Phan, B. M. Gerry, A. Kuhn, L. Z. Hong, Y. M. Ong, P. S. Y. Poon, M. A. Unger, R. C. Jones, S. R. Quake and W. F. Burkholder, *PLoS One*, 2013, **8**, e64084.
- 25 D. E. Discher, D. J. Mooney and P. W. Zandstra, *Science*, 2009, **324**, 1673–1677.
- 26 S. V. Murphy and A. Atala, *Nat. Biotechnol.*, 2014, **32**, 773–785.
- 27 Y. Tan, D. J. Richards, T. C. Trusk, R. P. Visconti, M. J. Yost, M. S. Kindy, C. J. Drake, W. S. Argraves, R. R. Markwald and Y. Mei, *Biofabrication*, 2014, **6**, 024111.
- 28 M. Gupta, F. Meng, B. Johnson, Y. L. Kong, L. Tian, Y.-W. Yeh, N. Masters, S. Singamaneni and M. C. McAlpine, *Nano Lett.*, 2015, DOI: 10.1021/acs.nanolett.5b01688.

- 29 S. Guven, P. Chen, F. Inci, S. Tasoglu, B. Erkmén and U. Demirci, *Trends Biotechnol.*, 2015, **33**, 269–279.
- 30 D. An, Y. Ji, A. Chiu, Y.-C. Lu, W. Song, L. Zhai, L. Qi, D. Luo and M. Ma, *Biomaterials*, 2015, **37**, 40–48.
- 31 G. Orive, R. M. Hernández, A. R. Gascón, R. Calafiore, T. M. Chang, P. De Vos, G. Hortelano, D. Hunkeler, I. Lacík, A. J. Shapiro and J. L. Pedraz, *Nat. Med.*, 2003, **9**, 104–107.
- 32 B. Buder, M. Alexander, R. Krishnan, D. W. Chapman and J. R. Lakey, *Immune Netw.*, 2013, **13**, 235–239.
- 33 R. M. Schoeman, E. W. Kemna, F. Wolbers and A. Berg, *Electrophoresis*, 2014, **35**, 385–392.
- 34 Y. Qu, N. Hu, H. Xu, J. Yang, B. Xia, X. Zheng and Z. Q. Yin, *Microfluid. Nanofluid.*, 2011, **11**, 633–641.
- 35 A. M. Skelley, O. Kirak, H. Suh, R. Jaenisch and J. Voldman, *Nat. Methods*, 2009, **6**, 147–152.
- 36 A. Huebner, M. Srisa-Art, D. Holt, C. Abell, F. Hollfelder, A. deMello and J. Edel, *Chem. Commun.*, 2007, 1218–1220.
- 37 L. Mazutis, J. Gilbert, W. L. Ung, D. A. Weitz, A. D. Griffiths and J. A. Heyman, *Nat. Protoc.*, 2013, **8**, 870–891.
- 38 S.-Y. Teh, R. Lin, L.-H. Hung and A. P. Lee, *Lab Chip*, 2008, **8**, 198–220.
- 39 M. T. Guo, A. Rotem, J. A. Heyman and D. A. Weitz, *Lab Chip*, 2012, **12**, 2146–2155.
- 40 E. Brouzes, M. Medkova, N. Savenelli, D. Marran, M. Twardowski, J. B. Hutchison, J. M. Rothberg, D. R. Link, N. Perrimon and M. L. Samuels, *Proc. Natl. Acad. Sci. U. S. A.*, 2009, **106**, 14195–14200.
- 41 Y.-J. Eun, A. S. Utada, M. F. Copeland, S. Takeuchi and D. B. Weibel, *ACS Chem. Biol.*, 2010, **6**, 260–266.
- 42 P. C. Blainey, *FEMS Microbiol. Rev.*, 2013, **37**, 407–427.
- 43 C. E. Stanley, R. C. Wootton and A. J. deMello, *Chimia*, 2012, **66**, 88–98.
- 44 O. J. Dressler, R. M. Maceiczky, S.-I. Chang and A. J. deMello, *J. Biomol. Screening*, 2014, **19**, 483–496.
- 45 M. Sesen, T. Alan and A. Neild, *Lab Chip*, 2014, **14**, 3325–3333.
- 46 B. Teste, N. Jamond, D. Ferraro, J.-L. Viovy and L. Malaquin, *Microfluid. Nanofluid.*, 2015, 1–13.
- 47 E. Um, E. Rha, S.-L. Choi, S.-G. Lee and J.-K. Park, *Lab Chip*, 2012, **12**, 1594–1597.
- 48 H. Song, D. L. Chen and R. F. Ismagilov, *Angew. Chem., Int. Ed.*, 2006, **45**, 7336–7356.
- 49 L. Mazutis and A. D. Griffiths, *Lab Chip*, 2012, **12**, 1800–1806.
- 50 Z. Li, K. Ando, J. Yu, A. Liu, J. Zhang and C. Ohl, *Lab Chip*, 2011, **11**, 1879–1885.
- 51 M. He, C. Sun and D. T. Chiu, *Anal. Chem.*, 2004, **76**, 1222–1227.
- 52 P. Mary, V. Studer and P. Tabeling, *Anal. Chem.*, 2008, **80**, 2680–2687.
- 53 S. Berger, J. Stawikowska, D. van Swaay and A. deMello, *Ind. Eng. Chem. Res.*, 2014, **53**, 9256–9261.
- 54 Y. Bai, E. Weibull, H. N. Joensson and H. Andersson-Svahn, *Sens. Actuators, B*, 2014, **194**, 249–254.
- 55 T. Nisisako, S. A. Portonovo and J. J. Schmidt, *Analyst*, 2013, **138**, 6793–6800.
- 56 Y. Elani, A. J. deMello, X. Niu and O. Ces, *Lab Chip*, 2012, **12**, 3514–3520.
- 57 Y. Bai, X. He, D. Liu, S. N. Patil, D. Bratton, A. Huebner, F. Hollfelder, C. Abell and W. T. S. Huck, *Lab Chip*, 2010, **10**, 1281–1285.
- 58 S. Cho, D.-K. Kang, S. Sim, F. Geier, J.-Y. Kim, X. Niu, J. B. Edel, S.-I. Chang, R. C. Wootton, K. S. Elvira and A. J. deMello, *Anal. Chem.*, 2013, **85**, 8866–8872.
- 59 A. Huebner, D. Bratton, G. Whyte, A. J. deMello, M. Yang, C. Abell and F. Hollfelder, *Lab Chip*, 2009, **9**, 692–698.
- 60 T. Schneider, J. Kreutz and D. T. Chiu, *Anal. Chem.*, 2013, **85**, 3476–3482.
- 61 A. Rakszewska, J. Tel, V. Chokkalingam and W. T. Huck, *NPG Asia Mater.*, 2014, **6**, e133.
- 62 X. Niu and A. J. deMello, *Biochem. Soc. Trans.*, 2012, **40**, 615–623.
- 63 S. Juul, Y.-P. Ho, J. Koch, F. F. Andersen, M. Stougaard, K. W. Leong and B. R. Knudsen, *ACS Nano*, 2011, **5**, 8305–8310.
- 64 P. Kumaresan, C. J. Yang, S. A. Cronier, R. G. Blazej and R. A. Mathies, *Anal. Chem.*, 2008, **80**, 3522–3529.
- 65 J. J. Agresti, E. Antipov, A. R. Abate, K. Ahn, A. C. Rowat, J.-C. Baret, M. Marquez, A. M. Klibanov, A. D. Griffiths and D. A. Weitz, *Proc. Natl. Acad. Sci. U. S. A.*, 2010, **107**, 4004–4009.
- 66 A. Zinchenko, S. R. Devenish, B. Kintses, P.-Y. Colin, M. Fischlechner and F. Hollfelder, *Anal. Chem.*, 2014, **86**, 2526–2533.
- 67 B. Kintses, C. Hein, M. F. Mohamed, M. Fischlechner, F. Courtois, C. Lainé and F. Hollfelder, *Chem. Biol.*, 2012, **19**, 1001–1009.
- 68 A. Fallah-Araghi, J.-C. Baret, M. Ryckelynck and A. D. Griffiths, *Lab Chip*, 2012, **12**, 882–891.
- 69 H. Yamaguchi, M. Maeki, K. Yamashita, H. Nakamura, M. Miyazaki and H. Maeda, *J. Biochem.*, 2013, **153**, 339–346.
- 70 I. Lignos, L. Protesescu, S. Stavrakis, L. Piveteau, M. J. Speirs, M. A. Loi, M. V. Kovalenko and A. J. deMello, *Chem. Mater.*, 2014, **26**, 2975–2982.
- 71 M. Srisa-Art, A. J. deMello and J. B. Edel, *J. Phys. Chem. B*, 2010, **114**, 15766–15772.
- 72 J.-W. Choi, D.-K. Kang, H. Park, A. J. deMello and S.-I. Chang, *Anal. Chem.*, 2012, **84**, 3849–3854.
- 73 Y. Song, J. Hormes and C. S. Kumar, *Small*, 2008, **4**, 698–711.
- 74 C.-X. Zhao, *Adv. Drug Delivery Rev.*, 2013, **65**, 1420–1446.
- 75 A. B. Theberge, F. Courtois, Y. Schaerli, M. Fischlechner, C. Abell, F. Hollfelder and W. T. Huck, *Angew. Chem., Int. Ed.*, 2010, **49**, 5846–5868.
- 76 H. N. Joensson and H. Andersson Svahn, *Angew. Chem., Int. Ed.*, 2012, **51**, 12176–12192.
- 77 S. Köster, F. E. Angile, H. Duan, J. J. Agresti, A. Wintner, C. Schmitz, A. C. Rowat, C. A. Merten, D. Pisignano, A. D. Griffiths and D. A. Weitz, *Lab Chip*, 2008, **8**, 1110–1115.
- 78 J. Clausell-Tormos, D. Lieber, J.-C. Baret, A. El-Harrak, O. J. Miller, L. Frenz, J. Blouwolf, K. J. Humphry, S. Köster, H. Duan, C. Holtze, D. A. Weitz, A. D. Griffiths and C. A. Merten, *Chem. Biol.*, 2008, **15**, 427–437.

- 79 A. Kang, J. Park, J. Ju, G. S. Jeong and S.-H. Lee, *Biomaterials*, 2014, **35**, 2651–2663.
- 80 T. P. Lagus and J. F. Edd, *J. Phys. D: Appl. Phys.*, 2013, **46**, 114005.
- 81 T. Tran, F. Lan, C. Thompson and A. Abate, *J. Phys. D: Appl. Phys.*, 2013, **46**, 114004.
- 82 L. Adams, T. E. Kodger, S.-H. Kim, H. C. Shum, T. Franke and D. A. Weitz, *Soft Matter*, 2012, **8**, 10719–10724.
- 83 S. L. Anna, N. Bontoux and H. A. Stone, *Appl. Phys. Lett.*, 2003, **82**, 364–366.
- 84 H. Song, M. R. Bringer, J. D. Tice, C. J. Gerdtz and R. F. Ismagilov, *Appl. Phys. Lett.*, 2003, **83**, 4664–4666.
- 85 T. Nisisako, T. Torii and T. Higuchi, *SICE*, 2002, pp. 957–959.
- 86 T. Thorsen, R. W. Roberts, F. H. Arnold and S. R. Quake, *Phys. Rev. Lett.*, 2001, **86**, 4163.
- 87 J.-U. Shim, R. T. Ransinghe, C. A. Smith, S. M. Ibrahim, F. Hollfelder, W. T. Huck, D. Klenerman and C. Abell, *ACS Nano*, 2013, **7**, 5955–5964.
- 88 C.-X. Zhao and A. P. Middelberg, *Chem. Eng. Sci.*, 2011, **66**, 1394–1411.
- 89 C. N. Baroud, F. Gallaire and R. Dangla, *Lab Chip*, 2010, **10**, 2032–2045.
- 90 Y. Ding, X. C. i Solvas and A. deMello, *Analyst*, 2015, **140**, 414–421.
- 91 J. Hong, M. Choi, J. B. Edel and A. J. deMello, *Lab Chip*, 2010, **10**, 2702–2709.
- 92 S.-K. Chae, C.-H. Lee, S. H. Lee, T.-S. Kim and J. Y. Kang, *Lab Chip*, 2009, **9**, 1957–1961.
- 93 W.-A. C. Bauer, M. Fischlechner, C. Abell and W. T. Huck, *Lab Chip*, 2010, **10**, 1814–1819.
- 94 G. Christopher and S. Anna, *J. Phys. D: Appl. Phys.*, 2007, **40**, R319.
- 95 M. De Menech, P. Garstecki, F. Jousse and H. Stone, *J. Fluid Mech.*, 2008, **595**, 141–161.
- 96 Z. Nie, M. Seo, S. Xu, P. C. Lewis, M. Mok, E. Kumacheva, G. M. Whitesides, P. Garstecki and H. A. Stone, *Microfluid. Nanofluid.*, 2008, **5**, 585–594.
- 97 Q. Xu and M. Nakajima, *Appl. Phys. Lett.*, 2004, **85**, 3726–3728.
- 98 S. Häberle, R. Zengerle and J. Duerée, *Microfluid. Nanofluid.*, 2007, **3**, 65–75.
- 99 M. He, J. S. Kuo and D. T. Chiu, *Appl. Phys. Lett.*, 2005, **87**, 031916.
- 100 Y. Zeng, M. Shin and T. Wang, *Lab Chip*, 2013, **13**, 267–273.
- 101 D. J. Collins, T. Alan, K. Helmersen and A. Neild, *Lab Chip*, 2013, **13**, 3225–3231.
- 102 S.-Y. Park, T.-H. Wu, Y. Chen, M. A. Teitell and P.-Y. Chiou, *Lab Chip*, 2011, **11**, 1010–1012.
- 103 L. Schmid and T. Franke, *Lab Chip*, 2013, **13**, 1691–1694.
- 104 L. Schmid and T. Franke, *Appl. Phys. Lett.*, 2014, **104**, 133501.
- 105 S. H. Tan, B. Semin and J.-C. Baret, *Lab Chip*, 2014, **14**, 1099–1106.
- 106 A. R. Abate, M. B. Romanowsky, J. J. Agresti and D. A. Weitz, *Appl. Phys. Lett.*, 2009, **94**, 023503.
- 107 V. Miralles, A. Huerre, H. Williams, B. Fournié and M.-C. Jullien, *Lab Chip*, 2015, **15**, 2133–2139.
- 108 P.-C. Hoa, Y.-F. Yap, N.-T. Nguyen and J. Chee-Kiong Chai, *Micro Nanosyst.*, 2011, **3**, 65–75.
- 109 S.-H. Tan, S. S. Murshed, N.-T. Nguyen, T. N. Wong and L. Yobas, *J. Phys. D: Appl. Phys.*, 2008, **41**, 165501.
- 110 N.-T. Nguyen, T.-H. Ting, Y.-F. Yap, T.-N. Wong, J. C.-K. Chai, W.-L. Ong, J. Zhou, S.-H. Tan and L. Yobas, *Appl. Phys. Lett.*, 2007, **91**, 084102.
- 111 S. Xiong, L. K. Chin, K. Ando, T. Tandiono, A.-Q. Liu and C.-D. Ohl, *Lab Chip*, 2015, **15**, 1451–1457.
- 112 J. Xu and D. Attinger, *J. Micromech. Microeng.*, 2008, **18**, 065020.
- 113 J. Choi, S. Lee, D. Lee, J. Kim, A. deMello and S. Chang, *RSC Adv.*, 2014, **4**, 20341–20345.
- 114 J. Hong, A. deMello and S. N. Jayasinghe, *Biomed. Mater.*, 2010, **5**, 021001.
- 115 D. Moon, D. J. Im, S. Lee and I. S. Kang, *Exp. Therm. Fluid Sci.*, 2014, **53**, 251–258.
- 116 U. Tangen, A. Sharma, P. Wagler and J. S. McCaskill, *Biomicrofluidics*, 2015, **9**, 014119.
- 117 R. M. Lorenz, J. S. Edgar, G. D. Jeffries and D. T. Chiu, *Anal. Chem.*, 2006, **78**, 6433–6439.
- 118 E. Castro-Hernández, P. García-Sánchez, S. H. Tan, A. M. Gañán-Calvo, J.-C. Baret and A. Ramos, *Microfluid. Nanofluid.*, 2015, 1–8.
- 119 C. N. Baroud, M. R. de Saint Vincent and J.-P. Delville, *Lab Chip*, 2007, **7**, 1029–1033.
- 120 C. N. Baroud, J.-P. Delville, F. Gallaire and R. Wunenburger, *Phys. Rev. E: Stat., Nonlinear, Soft Matter Phys.*, 2007, **75**, 046302.
- 121 S.-K. Hsiung, C.-T. Chen and G.-B. Lee, *J. Micromech. Microeng.*, 2006, **16**, 2403.
- 122 H. Willaime, V. Barbier, L. Kloul, S. Maine and P. Tabeling, *Phys. Rev. Lett.*, 2006, **96**, 054501.
- 123 C.-T. Chen and G.-B. Lee, *J. Microelectromech. Syst.*, 2006, **15**, 1492–1498.
- 124 H. Amini, W. Lee and D. Di Carlo, *Lab Chip*, 2014, **14**, 2739–2761.
- 125 D. Mark, S. Haeberle, G. Roth, F. von Stetten and R. Zengerle, *Chem. Soc. Rev.*, 2010, **39**, 1153–1182.
- 126 R. Seemann, M. Brinkmann, T. Pfohl and S. Herminghaus, *Rep. Prog. Phys.*, 2012, **75**, 016601.
- 127 J. M. Martel and M. Toner, *Annu. Rev. Biomed. Eng.*, 2014, **16**, 371–396.
- 128 J. Yu, W. Huang, L. K. Chin, L. Lei, Z. Lin, W. Ser, H. Chen, T. C. Ayi, P. H. Yap, C. H. Chen and A. Q. Liu, *Lab Chip*, 2014, **14**, 3519–3524.
- 129 M. Najah, A. D. Griffiths and M. Ryckelynck, *Anal. Chem.*, 2012, **84**, 1202–1209.
- 130 H. Wang, W. Zhang and Z. Dai, *Anal. Methods*, 2014, **6**, 9754–9760.
- 131 S. Haeberle, L. Naegel, R. Burger, F. V. Stetten, R. Zengerle and J. Duerée, *J. Microencapsulation*, 2008, **25**, 267–274.
- 132 H. Onoe, K. Inamori, M. Takinoue and S. Takeuchi, *RSC Adv.*, 2014, **4**, 30480–30484.

- 133 A. Chen, T. Byvank, W.-J. Chang, A. Bharde, G. Vieira, B. L. Miller, J. J. Chalmers, R. Bashir and R. Sooryakumar, *Lab Chip*, 2013, **13**, 1172–1181.
- 134 D. J. Collins, T. Alan and A. Neild, *Appl. Phys. Lett.*, 2014, **105**, 033509.
- 135 E. Brouzes, T. Kruse, R. Kimmerling and H. H. Strey, *Lab Chip*, 2015, **15**, 908–919.
- 136 B. Verbruggen, T. Tóth, M. Cornaglia, R. Puers, M. A. Gijs and J. Lammertyn, *Microfluid. Nanofluid.*, 2014, **18**, 91–102.
- 137 M. He, J. S. Edgar, G. D. Jeffries, R. M. Lorenz, J. P. Shelby and D. T. Chiu, *Anal. Chem.*, 2005, **77**, 1539–1544.
- 138 T.-H. Wu, Y. Chen, S.-Y. Park, J. Hong, T. Teslaa, J. F. Zhong, D. Di Carlo, M. A. Teitell and P.-Y. Chiou, *Lab Chip*, 2012, **12**, 1378–1383.
- 139 T. Franke, S. Braunmüller, L. Schmid, A. Wixforth and D. Weitz, *Lab Chip*, 2010, **10**, 789–794.
- 140 L. Schmid, D. A. Weitz and T. Franke, *Lab Chip*, 2014, **14**, 3710–3718.
- 141 P.-Y. Chiou, T.-H. S. Wu, S.-Y. Park and M. A. Teitell, High-speed on demand droplet generation and single cell encapsulation driven by induced cavitation, *US Pat.*, 2012, App. 13/370,196.
- 142 J.-C. Baret, O. J. Miller, V. Taly, M. Ryckelynck, A. El-Harrak, L. Frenz, C. Rick, M. L. Samuels, J. B. Hutchison, J. J. Agresti, D. R. Link, D. A. Weitz and A. D. Griffiths, *Lab Chip*, 2009, **9**, 1850–1858.
- 143 J. Nam, H. Lim, C. Kim, J. Y. Kang and S. Shin, *Biomicrofluidics*, 2012, **6**, 024120.
- 144 J. McGrath, M. Jimenez and H. Bridle, *Lab Chip*, 2014, **14**, 4139–4158.
- 145 H. N. Joensson, M. Uhlén and H. A. Svahn, *Lab Chip*, 2011, **11**, 1305–1310.
- 146 T. Jing, R. Ramji, M. E. Warkiani, J. Han, C. T. Lim and C.-H. Chen, *Biosens. Bioelectron.*, 2015, **66**, 19–23.
- 147 M. Chabert and J.-L. Viovy, *Proc. Natl. Acad. Sci. U. S. A.*, 2008, **105**, 3191–3196.
- 148 E. Um, S.-G. Lee and J.-K. Park, *Appl. Phys. Lett.*, 2010, **97**, 153703.
- 149 J. F. Edd, D. Di Carlo, K. J. Humphry, S. Köster, D. Irimia, D. A. Weitz and M. Toner, *Lab Chip*, 2008, **8**, 1262–1264.
- 150 E. W. Kemna, R. M. Schoeman, F. Wolbers, I. Vermes, D. A. Weitz and A. van den Berg, *Lab Chip*, 2012, **12**, 2881–2887.
- 151 J. Schoendube, D. Wright, R. Zengerle and P. Koltay, *Biomicrofluidics*, 2015, **9**, 014117.
- 152 A. R. Abate, C.-H. Chen, J. J. Agresti and D. A. Weitz, *Lab Chip*, 2009, **9**, 2628–2631.
- 153 S. Seiffert, J. Thiele, A. R. Abate and D. A. Weitz, *J. Am. Chem. Soc.*, 2010, **132**, 6606–6609.
- 154 D. J. Collins, T. Alan and A. Neild, *Lab Chip*, 2014, **14**, 1595–1603.
- 155 Y. Ai, C. K. Sanders and B. L. Marrone, *Anal. Chem.*, 2013, **85**, 9126–9134.
- 156 G. Destgeer, B. H. Ha, J. Park, J. H. Jung, A. Alazzam and H. J. Sung, *Anal. Chem.*, 2015, **87**, 4627–4632.
- 157 V. Skowronek, R. W. Rambach and T. Franke, *Microfluid. Nanofluid.*, 2015, 1–7.
- 158 G. Destgeer, B. H. Ha, J. H. Jung and H. J. Sung, *Lab Chip*, 2014, **14**, 4665–4672.
- 159 B. Landenberger, H. Höfemann, S. Wadle and A. Rohrbach, *Lab Chip*, 2012, **12**, 3177–3183.
- 160 M. MacDonald, G. Spalding and K. Dholakia, *Nature*, 2003, **426**, 421–424.
- 161 O. Brzobohatý, V. Karásek, M. Šiler, L. Chvátal, T. Čížmár and P. Zemánek, *Nat. Photonics*, 2013, **7**, 123–127.
- 162 J. DuBose, J. Zhu, S. Patel, X. Lu, N. Tupper, J. M. Stonaker and X. Xuan, *J. Micromech. Microeng.*, 2014, **24**, 115018.
- 163 Y. Kang, D. Li, S. A. Kalams and J. E. Eid, *Biomed. Microdevices*, 2008, **10**, 243–249.
- 164 L. R. Huang, E. C. Cox, R. H. Austin and J. C. Sturm, *Science*, 2004, **304**, 987–990.
- 165 A. A. S. Bhagat, S. S. Kuntaegowdanahalli and I. Papautsky, *Lab Chip*, 2008, **8**, 1906–1914.
- 166 S. Li, X. Ding, F. Guo, Y. Chen, M. I. Lapsley, S.-C. S. Lin, L. Wang, J. P. McCoy, C. E. Cameron and T. J. Huang, *Anal. Chem.*, 2013, **85**, 5468–5474.
- 167 L. Wu, P. Chen, Y. Dong, X. Feng and B.-F. Liu, *Biomed. Microdevices*, 2013, **15**, 553–560.
- 168 R. Ostafe, R. Prodanovic, W. L. Ung, D. A. Weitz and R. Fischer, *Biomicrofluidics*, 2014, **8**, 041102.
- 169 T. C. Scanlon, S. M. Dostal and K. E. Griswold, *Biotechnol. Bioeng.*, 2014, **111**, 232–243.
- 170 M. Srisa-Art, I. C. Bonzani, A. Williams, M. M. Stevens, A. J. deMello and J. B. Edel, *Analyst*, 2009, **134**, 2239–2245.
- 171 J. Cao, S. Nagl, E. Kothe and J. M. Köhler, *Microchim. Acta*, 2015, **182**, 385–394.
- 172 G.-S. Du, J.-Z. Pan, S.-P. Zhao, Y. Zhu, J. M. den Toonder and Q. Fang, *Anal. Chem.*, 2013, **85**, 6740–6747.
- 173 L. Galla, D. Greif, J. Regtmeier and D. Anselmetti, *Biomicrofluidics*, 2012, **6**, 014104.
- 174 Y. Zhu and Q. Fang, *Anal. Chim. Acta*, 2013, **787**, 24–35.
- 175 E. W. Kemna, L. I. Segerink, F. Wolbers, I. Vermes and A. van den Berg, *Analyst*, 2013, **138**, 4585–4592.
- 176 L. M. Fidalgo, G. Whyte, B. T. Ruotolo, J. L. Benesch, F. Stengel, C. Abell, C. V. Robinson and W. T. Huck, *Angew. Chem., Int. Ed.*, 2009, **48**, 3665–3668.
- 177 C. A. Smith, X. Li, T. H. Mize, T. D. Sharpe, E. I. Graziani, C. Abell and W. T. Huck, *Anal. Chem.*, 2013, **85**, 3812–3816.
- 178 E. Zang, S. Brandes, M. Tovar, K. Martin, F. Mech, P. Horbert, T. Henkel, M. T. Figge and M. Roth, *Lab Chip*, 2013, **13**, 3707–3713.
- 179 S. Numakunai, A. Jamsaid, D. H. Yoon, T. Sekiguchi and S. Shoji, *Micro Electro Mechanical Systems (MEMS), 2014 IEEE 27th International Conference on*, 2014, pp. 92–95.
- 180 Y. Harada, D. H. Yoon, T. Sekiguchi and S. Shoji, *Micro Electro Mechanical Systems (MEMS), 2012 IEEE 25th International Conference on*, 2012, pp. 1105–1108.
- 181 Y.-C. Tan, Y. L. Ho and A. P. Lee, *Microfluid. Nanofluid.*, 2008, **4**, 343–348.
- 182 K. V. Rozhdestvensky, *Prog. Aeronaut. Sci.*, 2006, **42**, 211–283.
- 183 D. Di Carlo, *Lab Chip*, 2009, **9**, 3038–3046.
- 184 J. Oakey, R. W. Applegate Jr, E. Arellano, D. D. Carlo, S. W. Graves and M. Toner, *Anal. Chem.*, 2010, **82**, 3862–3867.

- 185 W. Lee, H. Amini, H. A. Stone and D. Di Carlo, *Proc. Natl. Acad. Sci. U. S. A.*, 2010, **107**, 22413–22418.
- 186 J.-P. Matas, V. Glezer, É. Guazzelli and J. F. Morris, *Phys. Fluids*, 2004, **16**, 4192–4195.
- 187 T. P. Lagus and J. F. Edd, *RSC Adv.*, 2013, **3**, 20512–20522.
- 188 I. Leibacher, J. Schoendube, J. Dual, R. Zengerle and P. Koltay, *Biomicrofluidics*, 2015, **9**, 024109.
- 189 A. Yusof, H. Keegan, C. D. Spillane, O. M. Sheils, C. M. Martin, J. J. O'Leary, R. Zengerle and P. Koltay, *Lab Chip*, 2011, **11**, 2447–2454.
- 190 A. Gross, J. Schöndube, S. Niekrawitz, W. Streule, L. Riegger, R. Zengerle and P. Koltay, *J. Lab. Autom.*, 2013, **18**, 504–518.
- 191 S. Allazetta, T. C. Hausherr and M. P. Lutolf, *Biomacromolecules*, 2013, **14**, 1122–1131.
- 192 T.-Y. Cheng, M.-H. Chen, W.-H. Chang, M.-Y. Huang and T.-W. Wang, *Biomaterials*, 2013, **34**, 2005–2016.
- 193 A. Khademhosseini and R. Langer, *Biomaterials*, 2007, **28**, 5087–5092.
- 194 S. Mazzitelli, L. Capretto, F. Quinci, R. Piva and C. Nastruzzi, *Adv. Drug Delivery Rev.*, 2013, **65**, 1533–1555.
- 195 B. G. Chung, K.-H. Lee, A. Khademhosseini and S.-H. Lee, *Lab Chip*, 2012, **12**, 45–59.
- 196 Y.-H. Lin, Y.-W. Yang, Y.-D. Chen, S.-S. Wang, Y.-H. Chang and M.-H. Wu, *Lab Chip*, 2012, **12**, 1164–1173.
- 197 P. Agarwal, S. Zhao, P. Bielecki, W. Rao, J. K. Choi, Y. Zhao, J. Yu, W. Zhang and X. He, *Lab Chip*, 2013, **13**, 4525–4533.
- 198 J. Wan, *Polymers*, 2012, **4**, 1084–1108.
- 199 M. Ma, A. Chiu, G. Sahay, J. C. Doloff, N. Dholakia, R. Thakrar, J. Cohen, A. Vegas, D. Chen, K. M. Bratlie, T. Dang, R. L. York, J. Hollister-Lock, G. C. Weir and D. G. Anderson, *Adv. Healthcare Mater.*, 2013, **2**, 667–672.
- 200 R. C. Kuhad, R. Gupta and A. Singh, *Enzyme Res.*, 2011, **2011**, 1–10.
- 201 T. Beneyton, F. Coldren, J.-C. Baret, A. D. Griffiths and V. Taly, *Analyst*, 2014, **139**, 3314–3323.
- 202 J. Shemesh, T. B. Arye, J. Avesar, J. H. Kang, A. Fine, M. Super, A. Meller, D. E. Ingber and S. Levenberg, *Proc. Natl. Acad. Sci. U. S. A.*, 2014, **111**, 11293–11298.
- 203 K. Shigeta, G. Koellensperger, E. Rampler, H. Traub, L. Rottmann, U. Panne, A. Okino and N. Jakubowski, *J. Anal. At. Spectrom.*, 2013, **28**(5), 637–645.
- 204 S. K. Küster, S. R. Fagerer, P. E. Verboket, K. Eyer, K. Jefimovs, R. Zenobi and P. S. Dittrich, *Anal. Chem.*, 2013, **85**(3), 1285–1289.